MOLYBDENUM-MODIFIED PLATINUM ELECTRODES

MOHAMMAD F. KHANFAR

Your file Votre référence
ISBN: 0-612-93036-X
Our file Notre référence
ISBN: 0-612-93036-X

Molybdenum-Modified Platinum Electrodes

By

Mohammad F. Khanfar

A thesis submitted to the School of Graduate Studies in partial fulfillment of the requirements for the degree of Master of Science

Department of Chemistry

Memorial University of Newfoundland

St.John's, Newfoundland, Canada

August 2003

Dedication

To my Mother, Sisters, and Brothers

Abstract

The modification of Pt electrodes with Mo compounds improves their catalytic activity toward the oxidation of methanol and formaldehyde in acidic solutions. The two sets of Mo oxides that have been studied in this work are the Hydrogen Molybdenum Bronze, H_xMoO_3, $0<x<2$, and the Molybdenum Oxides, MoO_x, $2<x<3$.

It has been found that the bronze $(H_2MoO_3)_{ads}$ is generated at the Pt surface in an *in situ* fashion upon the application of potentials more negative than 0 vs. Ag/AgCl. At higher positive potentials, the adsorbed bronze is oxidized to several intermediates that interact with methanol and facilitate its oxidation on the Pt surface. The nature of the interaction between the adsorbed intermediates and methanol needs further experimental investigation.

The deposition of MoO_3 on the surface of a commercial carbon supported Pt catalyst, has been achieved. The catalytic promotion observed with the modified catalyst over its unmodified counterpart has been explained in terms of the bi-functional mechanism introduced by Watanabe and Motoo. The activity of the Mo modified catalyst increases with the elevation of the MoO_3 surface concentration to a certain limit, then it decreases with further Mo addition. The extra MoO_3 content shields the Pt sites from the methanol or the formaldehyde molecules. In addition, it is added at the expense of the carbon content of the catalyst that is required for the electronic conductivity through the modified electrode.

Acknowledgments

I would like to express my deepest thanks and appreciation to Dr. Peter Pickup for his supervision and patience during the course of this work. I would also like to thank my supervisory committee, Dr. L. K. Thompson, and Dr. M. D. Mackey for their advice and guidance.

Special thanks to the members of Dr. Pickup's research group for their help, in particular, Dr. Omar Yépez and Dr. Chaojie Song. Thanks are also due to my friends in the departments of Chemistry, Biology, Physics, and Engineering.

Financial support from the Department of Chemistry, the School of Graduate Studies, and NSERC is also gratefully acknowledged.

Table of Contents

List of Abbreviations

AFM	Atomic Force Microscopy
AES	Auger Electron Spectroscopy
CF	Carbon Fiber
CV	Cyclic Voltammetry
DMFC	Direct Methanol Fuel Cell
EMIRS	Electromodulated Infrared Reflectance Spectroscopy
EDX	Electron Dispersive X-ray
Fc	Ferrocene
FTIR	Fourier Transform Infrared
GDMS	Glow-Discharge Mass Spectroscopy
HOPG	Highly Ordered Pyrolytic Graphite
LSV	Linear Scan Voltammogram
MEA	Membrane Electrode Assembly
MMS	Mercury Mercurous Sulfate
PEMFC	Proton Exchange Membrane Fuel Cell
RHE	Reference Hydrogen Electrode
RPM	Revolutions Per Minute
SCE	Saturated Calomel Electrode
SEM	Scanning Electron Microscopy
SHE	Standard Hydrogen Electrode
TGA	Thermal Gravimetric Analysis

TEM	Transmission Electron Microscopy
XRD	X Ray Diffraction
XPS	X-ray Photoelectron Spectroscopy

List of Figures

Chapter 2

Chapter 3

Chapter 4

Chapter 5

Chapter 1

Introduction

1.1 Significance of methanol as a promising fuel

On the industrial scale, methanol is generally produced from readily available substrates.[1] The organic liquid is usually synthesized by circulating a mixture of H_2, CO, and CO_2 in a loop over a $Cu/ZnO/Al_2O_3$ ternary catalyst. The process takes place at moderate temperatures (below 250 °C) and pressures (50 – 100 bar).

The production of methanol can be explained in terms of equations 1.1 to 1.3.

$$CO + 2H_2 \rightleftharpoons CH_3OH \quad (1.1)$$

$$CO_2 + 3\,H_2 \rightleftharpoons CH_3OH + H_2O \quad (1.2)$$

$$CO + H_2O \rightleftharpoons CO_2 + H_2 \quad (1.3)$$

Besides being easily prepared, methanol is conveniently transported, handled, and stored, and therefore, it can be supplied from distribution points for daily consumption.

Theses advantages qualify methanol to be utilized in fuel cell technology in direct methanol fuel cells (DMFC). A DMFC is a device that converts the chemical energy stored in methanol to electrical power. A DMFC is composed of three main parts, the anode, the electrolyte (which is usually a proton conducting polymer), and the cathode. In a DMFC, methanol is diluted with water, then the aqueous mixture is fed into the anode side of the cell.[2] Chemical energy is transformed into electrical energy as a

consequence of oxidation of the organic fuel, as shown by equation 1.4.

$$CH_3OH + H_2O \rightleftharpoons CO_2 + 6\,H^+ + 6\,e^- \quad (1.4)$$

Protons produced from the oxidation reaction migrate, through the proton-conducting membrane, to the cathode where oxygen is reduced as:

$$O_2 + 4H^+ + 4e^- \rightleftharpoons 2H_2O \quad (1.5)$$

Platinum is used as a catalyst for both of these reactions.

Platinum provides a catalytic surface for a wide range of electrochemical reactions in aqueous solutions. Pt is usually employed to perform electrode reactions with positive standard potentials.[3] Pt exhibits a significant activity for the oxidation of methanol, which is readily dissociated at the electrode surface, to produce stable adsorbed intermediates on the Pt surface.[4]

The oxidation of methanol to CO_2 on Pt starts with its adsorptive decomposition on the metal surface,[5] at potentials close to 0.20 V vs. RHE. C–H bond breaking is followed by several steps that end with the formation of adsorbed CO. Further oxidation of CO_{ads} to CO_2 requires the presence of an oxygen donor, usually adsorbed water molecules or OH groups. Activation of water by formation of adsorbed OH groups begins at about 0.45 V on Pt. Stripping of CO_{ads} therefore begins at approximately this potential. The process can be expressed by equations 1.6 to 1.8.

$$Pt + CH_3OH \rightleftharpoons Pt\text{–}CO + 4\,H^+ + 4e^- \quad (1.6)$$

$$Pt + H_2O \rightleftharpoons Pt - OH + H^+ + e^- \quad (1.7)$$

$$Pt - CO + Pt - OH \rightleftharpoons 2\,Pt + CO_2 + H^+ + e^- \quad (1.8)$$

Although the oxidation of methanol to CO_2 begins at ca. 0.45 V, useful oxidation rates

on pure Pt are only obtained at potentials above ca. 0.6 V. From a theoretical point of view, the oxidation of methanol as illustrated in equation 1.4 occurs at a standard potential of 0.046 V.[5] Thus, the oxidation reaction only takes place at a practical rate with the application of high overvoltages.

It has been found that the alloying of platinum with other transition metals, such as Ru, Sn, W, and Mo can enhance its catalytic activity toward methanol oxidation[6] by the formation of active oxygen donor species adsorbed onto the secondary metal. Formation of the active oxygen containing species occurs at lower potentials on these alloys. Their enhanced activity has been interpreted in terms of a bi–functional mechanism, proposed by Watanabe and Motoo,[7] where CO chemisorbed on Pt sites undergoes oxidative removal as shown in equation 1.9:

$$Pt\text{–}CO + M\text{–}OH \rightleftharpoons Pt + M + CO_2 + H^+ + e^- \qquad (1.9)$$

Here, M–OH is an oxygen containing species adsorbed on the secondary metallic sites.

In an effort to prove the bi-functional mechanism, as an explanation for the catalytic enhancement observed as a consequence of the alloying of Pt with the other transition metals, Watanabe and co-workers[8] studied the electro-oxidation of methanol on Pt and 50%Pt/50%Ru electrodes in acidic media. Linear scan voltammetric measurements showed that the oxidation of methanol on the binary alloy and on the Pt surface begins to increase at 0.4 V, and 0.6 V, respectively. Hence, the alloying of Pt with Ru decreases the oxidation overvoltage by ca. 0.2 V. These electrochemical measurements were coupled with *in situ* FTIR analysis. On the 50%Pt/50%Ru surface, IR bands due to the stretching and bending modes of adsorbed water were observed at 0.1 V

these bands were also observed for a pure Ru electrode but were absent from the IR spectra of pure Pt. It was therefore concluded that the adsorption of water molecules occurs at the Ru sites only, and that the adsorption process is followed by the formation of adsorbed hydroxyl groups on the Ru sites, as shown by equation 1.10:

$$Ru\text{-}OH_2 \rightleftharpoons Ru\text{-}OH + H^+ + e^- \qquad (1.10)$$

Pt is usually combined with other transition metals to form binary, ternary, or quaternary electrocatalysts. The catalysts take several forms, mainly as either unsupported alloys, or as alloy particles dispersed on a carbon or a polymeric support.

Besides the metal(s) added to Pt to obtain catalysts for methanol oxidation, the efficiency of the catalysts is affected by the synthetic route employed. Several of the methods that have been utilized to prepare catalysts for the anodic oxidation of methanol will be discussed in the following sections.

1.2 The oxidation of methanol on pure platinum

To investigate the nature of methanol electro-oxidation on Pt, electrodes with different surface structures have been employed. For example, Pt single crystal electrodes, mainly the Pt(100), Pt(110), and Pt(111) faces, are being widely used to study the kinetics and the mechanistic aspects of the oxidation reaction,[9] (in each single crystal plane, there is a unique, and an ordered repetition of a set of platinum atoms. The (111), (100), and the (110) correspond to a hexagonal, a square, and a rectangular arrangement of platinum atoms, respectively). On the other hand, polycrystalline Pt electrodes are generally used in experiments where the pH and temperature effects on the rate of

methanol oxidation are to be investigated.[10] The effects of preparation conditions on the catalyst structure, composition, and electrocatalytic activity are easily studied with the use of polymer and carbon supported Pt electrodes.[11,12]

The electro-oxidation of methanol on Pt single crystal electrodes with low Miller indexes, in different acidic media, has been studied by Herrero et al.[13] The oxidation of methanol on Pt(110), Pt(111), and Pt(100) was performed in $HClO_4$, H_2SO_4, and H_3PO_4 aqueous solutions. The reaction has been studied by means of cyclic voltammetry and chronoamperometry.

It has been found that the instantaneous methanol oxidation current (t = 0) depends on the surface geometry and on the electrolyte composition, and is unaffected by the formation of CO_{ads} that takes place during the course of the electrolysis. The highest methanol oxidation rate was found at Pt(110) in $HClO_4$, while the lowest rate was found at Pt(111) in H_3PO_4.

The variation in the catalytic activity of the three single-crystal surfaces was attributed to the different ratios between the edges or (defects), to the facets (or terraces), existing on each single crystal surface. As the edge to terrace ratio increases, the surface becomes more accessible for chemical adsorption processes; hence, it shows higher catalytic performance toward the oxidation of methanol. The order of reactivity of the three single crystal surfaces was found to be Pt(110) > Pt(100) > Pt(111), where the most catalytic surface has the highest edge to terrace ratio.

The effect of the electrolyte composition on the rate of methanol oxidation has been explained in terms of the anion adsorption strength, which was found to be in the

order of $H_2PO_4^- > HSO_4^- > ClO_4^-$. The adsorption of perchlorate, if it exists, takes place in regions where OH_{ads} is produced, at potentials more positive than the range where methanol oxidation occurs. In sulfuric and phosphoric acid aqueous solutions, adsorption of the sulfate or phosphate competes with methanol oxidation since adsorption of the counter anion and the oxidation of methanol occur in the same potential range.

Herrero et al[13] also reported that the formation of CO_{ads} occurs in a fashion similar to that reported for the oxidation of methanol; that is the highest poisoning effect occurs at Pt(110) in $HClO_4$ and the lowest effect at Pt(111) in H_3PO_4. The same explanation mentioned above, for the oxidation of methanol was used to account for the extent of poisoning by adsorbed carbon monoxide. Therefore, it was concluded that the problem of Pt deactivation couldn't be solved only by optimization of the surface structure and the electrolyte composition.

The oxidation of methanol on Pt(100), Pt(110), and Pt(111) in alkaline media has been reported by Tripković et al.[14] The oxidation reaction was found to be significantly dependent on the orientation of the electrode surface.

The first linear scans of the three planes, in CH_3OH/NaOH aqueous solution showed that Pt(111) is the most active plane, since the oxidation peak was 10 times greater than those generated from the oxidation of methanol on Pt(110) and Pt(100). This is despite the fact that the oxidation of methanol on Pt(111) starts at a more positive potential than the onset of methanol oxidation on Pt(100).

The difference in the catalytic activity between Pt(111) and the other two Pt electrodes was attributed to the formation of OH_{ads} groups on the Pt(111) surface. The

adsorbed hydroxyl groups participate in the oxidation, as shown by equations 1.11 to 1.14:

$$CH_3OH + OH^- \rightleftharpoons CH_3OH_{ads} + H_2O + e^- \quad (1.11)$$

$$CH_3O_{ads} + 3OH^- \rightleftharpoons CO_{ads} + 3H_2O + 3\,e^- \quad (1.12)$$

$$H_2O \rightleftharpoons OH_{ads} + H^+ + e^- \quad (1.13)$$

$$CO_{ads} + OH_{ads} \rightleftharpoons CO_2 + H^+ + e^- \quad (1.14)$$

The cyclic voltammograms of the three electrodes in NaOH aqueous solution showed that there is no evidence of the formation of OH_{ads} on Pt(100) below 0.8 V. A small peak was assigned to the formation of adsorbed hydroxyl groups on Pt(110). With Pt(111), however, the charge due to the formation of OH_{ads} corresponds to more than ½ of a monolayer of adsorbed OH species.

The oxidation reaction was tracked by FTIR measurements. The *in situ* FTIR spectroelectrochemical measurements of the oxidation of methanol in alkaline solution on the Pt(100) plane revealed the formation of linear and bridged forms of CO_{ads}. However, on Pt(111) only the presence of the linear-bonded form was detected. Tripković et al attributed the high catalytic activity of the Pt(111) plane, relative to the other two surfaces, to the least surface poisoning by CO_{ads}, and the higher methanol oxidation overpotential on this surface.

Cyclic voltammograms of Pt(111) and Pt(100), in CH_3OH/NaOH, showed that equivalent currents were generated during the anodic and the cathodic sweeps, indicating that under the experimental conditions employed, the electrolysis of methanol proceeds without the formation of strongly bound species. In acidic solutions, the situation is quite

different, as electrochemical features of the anodic and the cathodic scans are entirely different, as discussed below.

Li et al[15] reported the oxidation of methanol on a polycrystalline Pt electrode, in sulfuric acid. Cyclic voltammograms of the Pt electrode in CH_3OH/H_2SO_4 showed an oxidation peak generated during scanning in the positive direction, with a current maximum at ca. 0.8 V vs. SCE (ca. 1.0 V vs. SHE). The oxidation current was attributed to the formation of the intermediates shown in equations 1.15 to 1.18:

$$CH_3OH_{ads} \rightleftharpoons CH_3O_{ads} + H^+ + e^- \quad (1.15)$$

$$CH_3O_{ads} \rightleftharpoons CH_2O_{ads} + H^+ + e^- \quad (1.16)$$

$$CH_2O_{ads} \rightleftharpoons CHO_{ads} + H^+ + e^- \quad (1.17)$$

$$CHO_{ads} \rightleftharpoons CO_{ads} + H^+ + e^- \quad (1.18)$$

The current decreases at potentials more positive than 0.8 V until ca. 1 V. The depression in the current was attributed to the formation of surface Pt oxide as shown in equation 1.19:

$$Pt + H_2O \rightleftharpoons PtO + 2H^+ + 2e^- \quad (1.19)$$

The current increased again after 1 V until the end of the scan, mostly due to the direct oxidation of methanol to carbon dioxide on the oxide surface, as shown in equation 1.4. By switching the scan direction in the negative direction, the PtO was reduced as illustrated in equation 1.20:

$$PtO + 2H^+ + 2e^- \rightleftharpoons Pt + H_2O \quad (1.20)$$

The reduction process leaves a clean Pt surface; therefore, further oxidation of methanol to CO_2 occurs at the clean surface, with an oxidation peak at a lower potential.

Prabhuram and Monoharan[16] studied methanol oxidation on a porous Pt electrode in alkaline media. The working electrode was prepared by the chemical reduction of chloroplatinic acid (H_2PtCl_6) by $NaBH_4$. It was found that methanol oxidation on the unsupported Pt electrode in KOH aqueous solution depends on the CH_3OH/KOH molar ratio. The rate of methanol oxidation, tracked by cyclic voltammetry of the Pt electrode in several 1M CH_3OH/KOH mixtures, increases as the OH^- concentration increases from 1M to 6M. Above this limit, the remaining excess OH^-, after the oxidation of all adsorbed methanol molecules, retards the chemisorption of further methanol species at lower potentials.

Prabhuram and Monoharan reported that the highest rate of methanol oxidation on the Pt electrode occurs in a 6M CH_3OH + 6M KOH mixture. To account for this observation, they proposed the presence of an even distribution of adsorbed methanol and hydroxyl groups; therefore, the dissociatively adsorbed methanol, CH_3OH_{ads}, and adsorbed hydroxyl species cover adjacent Pt sites simultaneously. As a consequence, complete oxidation of the methanol takes place.

Carbon supported Pt powders were prepared by Lamy et al.[17] Two different commercial carbon substrates were used: graphite powder (HSAG 300) and carbon black (Vulcan XC-72). Before utilization, the HSAG 300 powder was oxidized with hot concentrated nitric acid to remove any metallic and/or organic impurities. The carbon black was used as received or was electrochemically oxidized in aqueous H_2SO_4.

The carbon support was mixed with Nafion® to produce an ink. A drop of the mixture was applied to the surface of a previously polished glassy carbon electrode, and

then the electrode was left to dry for a few hours at 80 °C. More details about preparation and utilization of the ink type electrodes can be found in Chapter 3.

Pt was electrochemically deposited on the carbon supports mentioned above by stepping the potential of the coated glassy carbon electrode in K_2PtCl_6/H_2SO_4 aqueous solution. Performances of the catalysts thus prepared toward methanol oxidation were assessed by conducting cyclic voltammetric measurements in aqueous CH_3OH/H_2SO_4 mixtures.

Lamy and co-workers found that the Pt specific activity toward the oxidation of methanol increases as the amount of surface oxides, obtained by treatment with concentrated HNO_3, on the carbon support surface increases. The enhancement was attributed to the presence of oxygenated species on the carbon surface; which in turn oxidize the adsorbed intermediates generated from the dissociative adsorption of methanol.

Polymer supported Pt catalysts were prepared by Bouzek et al.[18] Pt with different metal loadings was deposited on polypyrrole modified glassy carbon disc electrodes. Dispersion of the metal on the modified electrode was accomplished by the cathodic reduction of H_2PtCl_6 from an acidic aqueous solution, at 0.2 V vs. SCE.

Cyclic voltammograms of the prepared electrodes in CH_3OH/H_2SO_4, taken at a rotation rate of 1000 RPM, showed that with low Pt loadings (0.1-0.3 mg Pt/cm^2) an anodic peak appears near the end of the scan. This peak was attributed to an interaction between the polypyrrole and methanol or between the polypyrrole, methanol, and Pt. The reported peak vanishes at Pt loadings higher than 3.0 mg Pt/cm^2. To explain the

depression in the rate of methanol oxidation observed at high Pt loadings, Bouzek and co-workers proposed that at high Pt loadings, the deposited Pt islands merge into a compact Pt layer; consequently, they shield the polymer film from methanol.

The deposition of Pt on the polypyrrole modified glassy carbon electrode was repeated with different deposition potentials. Instead of 0.2 V the dispersion of Pt was performed potentiostatically at – 0.10 V. After the electrodeposition, cyclic voltammograms of the supported Pt electrodes in CH_3OH/H_2SO_4 were taken at 1000 RPM. The results showed that the rate of methanol oxidation is directly proportional to the Pt loading over a range of Pt loading from 0.2 to 0.5 mg Pt/cm^2. Bouzek et al concluded that with the electrodeposition at a more cathodic potential, the Pt islands form a less compact structure that does not isolate the polymer support from the aqueous solution.

1.3 Oxidation of methanol on Pt binary and ternary catalysts

Several Pt binary catalysts such as PtRu[19], PtOs[20], and PtSn[21] have been used. Their efficiency toward the oxidation of methanol has been examined with a wide range of different electrochemical and spectroscopic tools.

The activity of the secondary metal, incorporated with Pt, depends on its ability to produce oxygen-containing groups at potentials lower than that reported for Pt. According to the bi-functional mechanism, the adsorbed oxygenated species will accelerate the conversion of CO to CO_2 on Pt.

The structures of several PtRu catalysts and their catalytic activity toward methanol oxidation relative to their Pt counterparts have been extensively studied and correlated to the bi-functional mechanism.[22,23] The various electrodes that are discussed in section 1.2 have been alloyed with Ru. With unsupported Pt catalysts, Ru has been deposited on the surface of single crystal or polycrystalline Pt electrodes in the form of islands, decorating the Pt surface.[24,25]Carbon and polymer supported PtRu catalysts are usually obtained by simultaneous dispersion of the two metals on the support's surface.[26,27]

The deposition of Ru on Pt single crystal electrodes of low Miller indexes, namely Pt(100), Pt(110), and Pt(111), was performed by Tremiliosi-Filho et al.[28] Ru was deposited by holding the potential of the single crystal electrode at 0.3 V vs. RHE in $RuCl_3/HClO_4$ aqueous solution. The electrodes were characterized by Auger Electron Spectroscopy. For all of the electrodes prepared in this way, only a fraction of a monolayer of the surface was found to be decorated with Ru islands.

By conducting cyclic voltammetric experiments of the Ru decorated electrodes in $CH_3OH/HClO_4$, it was found that the highest methanol oxidation current was generated by the Pt(111)/Ru surface. Chronoamperometric measurements of methanol oxidation on the Pt(hkl)/Ru surfaces in CH_3OH/H_2SO_4 also showed that the highest steady state current was generated by the decorated Pt(111) surface.

Tremiliosi-Filho et al proposed that the catalytic activity of the Ru-modified single crystal electrodes, toward the oxidation of methanol, depends on the electrode's efficiency toward the oxidative removal of the poisoning CO, adsorbed on the Pt surface.

An interaction between an oxygenated Ru (RuO_x) and the poisoned Pt sites was proposed, as shown by equation 1.21:

$$Pt\text{-}CO + Pt/RuO_x \rightleftharpoons Pt + Pt/RuO_{x-1} + CO_2 \qquad (1.21)$$

It was postulated that the bimolecular reaction (equation 1.21) occurs on the smooth Ru alloyed Pt(111) surface faster than on the other single crystal Pt(hkl)/Ru electrodes, that contain defects and terraces. As the roughness of the Pt(hkl)/Ru increases, chemisorption of the O_x to the Ru site becomes weaker, allowing more oxygen site to site mobility and reactivity. Therefore, the concentration of the oxygenated Ru sites will decrease.

In addition to the effect of roughness of the surface, the effect of the heat of CO adsorption was also considered. The estimated heat of CO adsorption on Pt(111) is lower than that evolved by the adsorption of CO on Pt(110) and Pt(100). Therefore, the bimolecular reaction on the Pt(111) surface will be faster than on the other single crystal surfaces.

The deposition of Ru on a gold supported Pt black substrate was achieved by Waszczuk et al.[29] The procedure utilized by Tremiliosi-Filho et al, as mentioned above, was followed to prepare the binary catalyst. One of the main advantages of the deposition method is that the amount of deposited Ru can be controlled, therefore, PtRu catalysts with Ru densities increasing from 0.10 to 0.65 were prepared.

Catalytic activities of the PtRu catalysts as well as the undecorated Pt black, toward the electro-oxidation of methanol in CH_3OH/H_2SO_4, were assessed by chronoamperometry. Waszczuk et al[29] reported that the Ru free Pt black produces the

lowest steady state oxidation current, mostly due to the severe poisoning effect of the adsorbed CO generated from the oxidation of methanol, as shown in equation 1.22:

$$Pt + CH_3OH \rightleftharpoons Pt\text{-}CO + 4H^+ + 4e^- \quad (1.22)$$

With respect to the Ru decorated catalysts, the maximum activities at 0.30 and 0.40 V vs. RHE were reported with 0.40 and 0.50 ruthenium densities, respectively. Above these loadings, the steady state oxidation currents fall to lower values until the 0.65 Ru density was approached.

Waszczuk et al attributed the catalytic activity reported, upon the addition of Ru to the Pt black, to the enhancement of CO_{ads} oxidative removal, as explained by equation 1.23:

$$Pt\text{-}CO + Ru\text{-}OH \rightleftharpoons Pt + Ru + CO_2 + H^+ + e^- \quad (1.23)$$

The maximum catalytic effect was observed with catalysts of approximately 50:50 Pt:Ru surface ratio. This is considered as the optimal ratio as it provides room for the dissociative decomposition of methanol on the Pt sites. It also gives the maximum number of Ru-OH adsorbed sites required for the removal of CO_{ads}, as demonstrated by equation 1.23.

The oxidation of methanol on a carbon supported PtRu catalyst was studied by Tripković et al.[30] The catalytic activity of a commercial 54 mass % PtRu (with 2:3 Pt:Ru stoichiometric ratio) catalyst toward the oxidation of methanol in acidic and alkaline media was reported at 295 K and 333 K.

A common feature among cyclic voltammograms of the Pt_2Ru_3 catalyst in all of the studied aqueous solutions, at 295 K and at 333 K, is the presence of a fast increase in

the oxidation current, which is followed by an even faster drop in the current after a certain potential, to the end of the scan. To account for the reported behavior, Tripković et al proposed an equilibrium between methanol dissociation to CO_{ads}, and the oxidative removal of the adsorbed CO. The equilibria can be expressed by equations 1.24 to 1.26:

$$CH_3OH_{solution} \rightleftharpoons CH_3OH_{ads} \rightleftharpoons CO_{ads} + 4H^+ + 4\,e^- \quad (1.24)$$

The oxidative removal of CO_{ads} is pH dependent, hence; in acidic media it occurs as:

$$CO_{ads} + OH_{ads} \rightleftharpoons CO_2 + H^+ + e^- \quad (1.25)$$

And in alkaline solutions it occurs as:

$$CO_{ads} + 2OH_{ads} + 3OH^- \rightleftharpoons CO_3^{2-} + 2H_2O + e^- \quad (1.26)$$

At a constant temperature, and at the same potential value, cyclic voltammetric measurements showed that the current densities are much higher in NaOH than in H_2SO_4. The observation of lower current densities in the acidic medium was attributed to either the adsorption of the bisulfate anion on the electrode surface, resulting in the inhibition of the dissociative chemisorption of methanol, shown in equation 1.24; or to the replacement of OH_{ads} with $HSO_4^-{}_{ads}$. Hence, the conversion of CO into CO_2, shown by equation 1.25, will be retarded.

Tripković et al found significant temperature effects on cyclic voltammetry of the PtRu catalyst in both acidic and alkaline media. At 333 K, it was reported that the onset of the oxidation reaction was shifted toward more negative potentials when compared with the onset of the oxidation reaction at 295K. In addition, the peak of the oxidation current at 333 K was five times greater than that observed at 295 K. These changes were

attributed to enhancement of the kinetics of the adsorption/dehydrogenation steps shown in equation 1.24.

Chronoamperometric measurements of methanol oxidation on the PtRu catalyst were performed in both acidic and alkaline solutions at 295 K and at 333 K. In agreement with the cyclic voltammetric results, higher steady state oxidation currents were reported in the alkaline solution than in the acidic medium. In addition, the oxidation current measured at 333 K was about 5 times higher than that measured at 295 K, regardless of the pH of the solution.

Besides the oxidation of methanol on the different PtRu catalysts demonstrated above, the oxidation reaction was also performed with PtOs catalysts, as was reported by Gökağaç and Kennedy.[31] A series of carbon supported PtOs catalysts, with different Pt/Os ratios were prepared by the chemical reduction of H_2PtCl_6 and K_2OsCl_6 from their aqueous solutions, on a carbon support. The appropriate amounts of Pt and Os were deposited when formaldehyde was used as the reducing agent. Catalysts with 11%Pt/C, 10%Pt/C+1%Os/C, 9%Pt/C+2%Os/C, 8%Pt/C+3%Os/C, 7%Pt/C+4%Os/C, 6%Pt/C+5%Os/C, and 5%Pt/C+6%Os/C were prepared by the chemical reduction method.

The electrocatalytic activity of the catalysts, toward the oxidation of methanol, was estimated by means of chronoamperometric analysis. Oxidation of methanol showed that the 7%Pt/C+4%Os/C and 6%Pt/C+5%Os/C catalysts gave the highest oxidation currents, higher even than the current obtained from 11%Pt/C prepared under identical experimental conditions. It was concluded that the oxidation of methanol on PtOs

catalysts does not depend only on the nominal Pt/Os ratio. Several factors, such as particle size, crystallite distribution, surface composition, oxidation state of the metals, metal-metal and metal-support interactions, should also be considered.

TEM surface analysis showed that the 7%Pt/C+4%Os/C and the 6%Pt/C+5% Os/C catalysts contained smaller particles, as well as lower agglomeration than the other samples. As the active surface areas of these catalysts are the highest, they showed the highest catalytic activity toward methanol oxidation.

Cyclic voltammetric responses of the catalysts toward the oxidation of methanol fall into two sets. With 7%Pt/C+4%Os/C, 6%Pt/C+5%Os/C, and 5%Pt/C+6%Os/C, the oxidation of methanol was inhibited at higher positive potentials, due to the formation of Pt-oxide. With the other set of catalysts, the oxidation proceeded until the end of the scan. The occurrence of a rapid conversion of the inactive Pt-oxide to Pt_3-COH has been proposed, giving a chance for methanol adsorption and further oxidation to take place.

XPS screening revealed the presence of Pt(II) in all of the samples, mostly in the form of adsorbed Pt-oxide and/or hydroxide species. The Pt(0)/Pt(II) ratio was approximately 7:3; except for 7%Pt/C+4%Os/C and 6%Pt/C+5%Os/C, for which the ratios were 1:1 and 8:2, respectively. Gökağaç and Kennedy could not find a correlation between the Pt(0)/Pt(II) ratio, and the catalytic activity of a catalyst toward the oxidation of methanol. XPS is an *ex situ* technique and, therefore, it is difficult to predict the Pt(0)/Pt(II) ratio during the oxidation reaction.

Another piece of information that the XPS analysis provided was that the Pt/Os surface ratio was found on most of the catalysts to be different from the nominal ratio.

The most active catalysts, 7%Pt/C+4%Os/C and 6%Pt/C+5%Os/C, were found to contain 82:18 Pt:Os surface ratios. It was found that the catalytic activity decreases as the Os surface content exceeds 18%. The drop in activity was attributed to the formation of Os oxide that inhibits methanol adsorption and, as a consequence, decreases the rate of methanol oxidation.

The deposition of tin on the surface of a Pt sheet has been achieved by Abdel Rahim et al.[32] Sn was deposited from a $SnCl_3/H_2SO_4$ aqueous solution. The electrodeposition was performed by two different methods, potentiostatically and galvanostatically.

Cyclic voltammetry of the modified Pt electrode in aqueous CH_3OH/H_2SO_4 exhibited two peaks; a cathodic peak, I_{p1}, at 0.108 V, and an anodic peak, I_{p2}, at 0.223 V vs. MMS (Mercury Mercurous Sulfate, E = 0.680 V vs. SHE). The two peaks increased by a factor of 10, upon the addition of Sn.

The unmodified Pt electrode showed a dramatic deterioration with repeated cycling. The peak currents after the fiftieth cycle were only 38 % of the peak currents reported after the second cycle. In the presence of Sn, the peak currents after the fiftieth cycle were about 93% of the peak currents reported after the second cycle. The modified electrode showed only a slight loss in efficiency, when compared to the pure Pt electrode.

Abdel Rahim et al reported that the electroactivity of the PtSn surface alloy, toward the oxidation of methanol in sulfuric acid, depends on the deposition time. In both of the potentiostatic and the galvanostatic deposition methods, the current density during the forward scan, I_{p2}, increases with the deposition time to a certain limit. After that limit

the current density decreases with time. The decay was attributed to the blockage of the Pt active sites if the Sn/Pt ratio exceeds a certain value.

The effect of methanol concentration on the oxidation reaction has also been studied. It was found that the oxidation current and the oxidation potential, at I_{p2}, increases with methanol concentration. The shift in the peak potential was attributed to the additional potential needed for the oxidative removal of adsorbed contaminants; since the concentration of the poisoning adsorbate increases with elevation of the methanol concentration.

The effect of the scan rate on the oxidation of methanol, on the PtSn surface, revealed that the oxidation current, I_{p2}, is directly proportional to the square root of the sweep rate, indicating that methanol is brought to the electrode surface by diffusion. The oxidation potential, E_{p2}, also increases linearly with the square root of the scan rate, confirming that an extra potential is consumed in the removal of the surface contaminants.

The preparation of ternary catalysts for the oxidation of methanol was reported by Léger et al.[33] Pt, Ru, and a third metal were dispersed on a polyaniline modified gold electrode. The deposition of the metals was achieved by the electroreduction of the corresponding metal salts from their aqueous solutions at a fixed potential. The amount of the deposited metals was controlled chronocoloumetrically.

Chronoamperometric analysis of the catalysts in $CH_3OH/HClO_4$ solution showed that the PtRuMo catalyst exhibited the highest oxidation currents over the 0.400-0.550V vs. RHE potential range. for time intervals varying from 5 to 30 min. The enhanced

catalytic activity of the ternary catalyst has been attributed to the ability of molybdenum to split water molecules at lower potentials (relative to Ru even). Hence, it generates an adsorbed oxygenated species, most probably adsorbed hydroxyl groups, which in turn catalyze the oxidation of CO_{ads} to CO_2, as illustrated by the bi-functional mechanism. On the other hand, PtRuAu showed the lowest activity toward the oxidation of methanol. The low activity was attributed to the poor ability of gold to adsorb OH species.

PtRuCo, PtRuNi, and PtRuFe exhibited significant performances; however, they demonstrated an appreciable deterioration under the employed experimental conditions. With these materials, the reproducibility of the experiment was poor and their efficiencies toward the oxidation reaction decreased with time.

EDX analysis of the PtRuMo catalyst showed that the Mo content does not exceed 5%. Cyclic voltammetric experiments, performed with both PtRu and PtRuMo in $CH_3OH/HClO_4$, showed that the latter catalyst exhibits higher oxidation current densities, over the investigated potential range.

1.4 Electrochemistry of molybdenum oxide thin films

A significant enhancement of the rate of methanol oxidation on Pt black in the presence of molybdate, MoO_4^{2-}, was reported by Shropshire.[34] Investigation of the role of Mo compounds on the oxidation of methanol on Pt surfaces has since been performed by various other research groups.[35,36] In general, it has been found that molybdenum oxides, MoO_x, $2<x<3$, rather than elemental Mo are responsible for promotion of the catalytic efficiency of Pt. The role of molybdenum oxides in the oxidation of methanol on Pt

electrodes is discussed in Chapter 4. The structure, composition, and the electrochemical behavior of MoO_x have been studied by several groups,[37,38] with a significant contribution from Dong et al,[39] as will be shown below within the context of this section.

The electrochemical deposition of a non-stoichiometric, mixed valent, molybdenum oxide film has been performed by Dong and Wang.[40] The film has been deposited by cycling the potential of a carbon fiber (CF) microelectrode in a freshly prepared aqueous Na_2MoO_4/H_2SO_4 solution. SEM analysis of a film deposited on a glassy carbon electrode, under identical experimental conditions, revealed the presence of a uniform and compact blue film with a thickness of about 1 μm. XPS analysis of the film detected the presence of Mo(IV), Mo(V), and Mo(IV) ions.

Cyclic voltammograms of the thin film in H_2SO_4 solution exhibited a broad anodic peak and a narrow cathodic peak. The peak currents were both found proportional to the scan rate, indicating a voltammetric response from a thin layer, deposited on the working electrode surface. At scan rates lower than 50 mVs^{-1}, the anodic peak splits into two separate waves. The electrochemical activity of the mixed valent molybdenum oxide thin film was attributed to the reduction of molybdenum trioxide, MoO_3, to the blue hydrogen molybdenum bronzes, $H_{0.36}MoO_3$, and $H_{0.93}MoO_3$. This reduction is followed by the reoxidation of the bronzes to MoO_3, during anodic scanning of the potential.

Extension of the upper and/or the lower limits of the cyclic voltammogram of the molybdenum modified CF, in H_2SO_4 solution, toward more positive and/or negative values was performed by Wang et al.[41] It was found that the extension causes a shift in

the reduction and the oxidation peaks toward more negative and more positive potentials, respectively. In returning to the initial potential range, the reduction and oxidation peak potentials could not be restored to their initial potential values. It was therefore concluded that a change in the structure and/or the composition of the deposited molybdenum film took place as a consequence of the change of the scan potential range.

For further investigation of the nature of the electrochemical behavior of the non-stoichiometric molybdenum oxide film, Wang et al[41] conducted cyclic voltammogrammic measurements of the molybdenum film in a H_2SO_4 solution (50 % (v/v) water+ethanol mixture), in the presence and in the absence of ferrocene (Fc). It was found that by setting the lower limit of the scan at values less negative than – 0.60 V vs. SCE, no peak current could be observed, in the presence or the absence of Fc. On the other hand, by setting the lower limit to potentials more negative than –1.2 V, an oxidation peak appeared at about 0.3 V. This anodic peak has been attributed to the oxidation of Fc species, since the oxidation peak was absent from the cyclic voltammogram of the MoO_x/C in the Fc free solution. In addition to the oxidation peak, a reduction peak has been observed near –1.1 V. This peak was attributed to the reduction of the adsorbed molybdenum film, since it has also been reported in the absence of Fc. A cathodic peak, due to the reduction of Fc^+, was not observed under any experimental conditions.

Wang et al concluded that the oxidation of Fc depends on the extent of the reduction of the adsorbed film. After oxidation of the Fc species, the adsorbed layer

becomes an insulator, unless the lower limit of the scan is more negative than –1.2 V.

To account for the experimental observations, Wang and co-workers proposed the formation of an open structure adsorbed layer, during the course of reduction of the molybdenum oxide film. During the flow of electrons into the film, H_3O^+ ions also enter the film simultaneously, to compensate for the charge, converting the film from the anhydrous and compact form to an open structure array with pores filled with water and other species, including Fc. As a consequence, the film's conductivity is enhanced and it becomes able to oxidize Fc at higher positive potentials.

Wang et al utilized the open structure model to account for several other experimental observations. It was found that the oxidation peak for Fc on the molybdenum modified CF microelectrode is several times higher than that occurring at the bare CF surface. In addition, the oxidation peak was found to be directly proportional to the scan rate, indicating a non-diffusional controlled electrochemical process.

It was proposed that after reduction of the molybdate layer, and as a consequence, formation of the open structure, Fc species entered the reduced film and formed an intermediate of the formula $Fc_xH_yMoO_3$ or Fc_yMoO_{3-z}, by a chemisorption interaction: The concentration of Fc in the molybdenum layer therefore increases, causing a significant increase of the Fc oxidation peak during positive scanning. The presence of the chemisorbed Fc species in pores throughout the open structure accounts for the thin layer voltammetric response, which was observed in the dependence of the oxidation peak on the scan rate.

The presence of two different structural forms of electrochemically deposited molybdenum films has been supported by Lui et al.[42] Their molybdenum film was deposited on a HOPG (Highly Ordered Pyrolytic Graphite) electrode surface, by the electrodeposition procedure previously employed by Wang et al,[41] as mentioned above.

AFM images of the deposited molybdenum film have been taken after polarizing the film at 0.5 V, and then at -0.5 V, corresponding to the oxidized and the reduced forms of the deposited molybdenum oxide, respectively. The surface roughness of the molybdenum oxide film has been found to increase in going from the oxidized state to the reduced states. The electrochemically induced structural change has been found almost reversible, and has been attributed to the transition from a compact and anhydrous oxide film, to an open, and conductive hydrous structure, corresponding to the oxidized and the reduced forms, respectively.

1.5 Objectives of the thesis

In this work, the effect of Mo oxides on the catalytic activity of Pt electrodes toward the oxidation of methanol and formaldehyde has been studied. Several forms of polycrystalline Pt have been modified with MoO_x. The activity of the catalysts has been studied by cyclic voltammetry.

Chapter 3 focuses on the ink methodology as a convenient and a credible way to prepare supported Pt electrodes. The chapter also concentrates on the calculation of %Pt utilization and includes practical notes about the electrochemical pretreatment of glassy carbon electrodes.

The choice of electrode modification employed in Chapters 4 and 5 was based on a review of the literature that revealed three distinct approaches. The oxidation of methanol at a Pt surface decorated with adsorbed Mo was found to occur with no significant catalytic improvement over its Mo free analog.[35] Mo_{ads} can catalyze the conversion of only weakly adsorbed CO into CO_2, and the process occurs at higher positive potentials with no practical use. The second form of Mo compounds that were studied are the hydrogen molybdenum bronzes, H_xMoO_3, $0<x<2$.[15] Deposition of Mo oxide, MoO_x, $2<x<3$, on a carbon support with the assistance of a chemical method was also reported. The work in this thesis therefore focused on the use of hydrogen molybdenum bronzes and Mo oxides.[36,43]

In Chapter 4, the promotion of the catalytic activity obtained in the presence of H_xMoO_3 is reported. Several experiments have been performed to verify the enhancement of the efficiency of the molybdenum modified Pt electrodes toward the oxidation of methanol in acidic medium.

Chapter 5 described the deposition of MoO_3 on a commercial carbon supported Pt catalyst has been achieved. The performance of the modified catalyst toward the oxidation of methanol and formaldehyde is reported.

List of References

[1] Twigg, M. V. In *Catalyst Handbook*; Wolfe Publishing Ltd.; England, ***1989***, p 446.

[2] Carrette, L.; Friedrich, K. A.; Stimming, U. *Fuel Cells* ***2001***, *1*, 13-39.

[3] Komorsky-Lovrić, Š. In *Electroanalytical Methods*; Scholz, F., Ed.; Springer-Verlag, Berlin, ***2002***, p 247.

[4] Hamnett, A. In *Interfacial Electrochemistry. Theory, Experimental, and Applications*, Wieckowski, A., Ed.; Marcel Dekker, NewYork, ***1999***, P844.

[5] Iwasita, T. *Electrochim. Acta* ***2002***, *47*, 3663-3674.

[6] Carrette, L.; Friedrich, K. A.; Stimming, U. *ChemPhysChem* ***2000***, *1*, 163-193.

[7] Watanabe, M.; Motoo, S. *Electroanal. Chem.* ***1975***, *60*, 267-273.

[8] Yajima, T.; Wakabayashi, N.; Uchida, H.; Watanabe, M. *Chem. Commun.* ***2003***, *7*, 828-829.

[9] Lebedeva, N. P.; Koper, M. T. M.; Feliu, J. M.; Santen, R. A. *J. Phys .Chem. B* ***2002***, *106*, 12938-12947.

[10] Kardash, D.; Korzeniewski, C. *Langmuir* ***2000***, *16*, 8419-8425.

[11] Stoyanova, A.; Naidenov, V.; Petrov, K.; Nikolov, I.; Vitanov, T.; Budevski, E. *J. Appl. Electrochem.* ***1999***, *29*, 1197-1203.

[12] Luna, A. M. C. *J. Appl. Electrochem.* ***2000***, *30*, 1137-1142.

[13] Herrero, E.; Franaszczuk, K.; Wieckowski, A. *J. Phys. Chem.* ***1994***, *98*, 5074-5083.

[14] Tripković, A. V.; Marinković, N.; Popović, K. Dj.; Adžić, R. R. *R. J. Electrochem.* ***1995***, *31*, 993-1003.

[15] Li, W. S.; Tian, L. P.; Huang, Q. M.; Li, H.; Chen, H. Y.; Lian, X . P. *J. Power Sources* ***2002***, *104*, 281-288.

[16] Prabhuram, J.; Manoharan, R. *J. Power Sources* ***1998***, *74*, 54-61.

[17] Gloaguen, F.; Léger,. J.-M.; Lamy, C. *J. Appl. Electrochem.* ***1997***, *27*, 1052-1060.

[18] Bouzek, K.; Mangold, K.-M.; Jüttner, K. *J. Appl. Electrochem.* ***2001***, *31*, 501-507.

[19] Neergat, M.; Leveratto, D.; Stimming, U. *Fuel Cells* ***2002***, *2*, 25-30.

[20] Crown, A.; Moraes, I. R.; Wieckowski, A. *J. Electroanal. Chem.* ***2001***, *500*, 333-343.

[21] Crabb, E. M.; Marshal, R.; Thompsett; D. *J. Electrochem. Soc.* ***2000***, *147*, 4440-4447.

[22] Lee, C. E.; Bergens, S. H. *J. Phys. Chem. B* ***1998***, *102*, 193-199.

[23] Fujiwara, N.; Yasuda, K.; Ioroi, T.; Siroma, Z.; Miyazaki, Y. *Electrochim. Acta* ***2002***, *47*, 4079-4084.

[24] Schmidt, T. J.; Noeske, M.; Gasteiger, H. A.; Behm, R. J. *Langmuir* ***1997***, *13*, 2591-2595.

[25] Waszczuk, P.; Lu, G.-Q.; Wieckowski, A.; Lu, C.; Rice, C.; Masel, R. I. *Electrochim. Acta* ***2002***, *47*, 3637-3652.

[26] Baldauf, M.; Preidel, W. *J. Appl. Electrochem.* ***2001***, *31*, 781-786.

[27] Steigerwait, E. S.; Deluga, G. A.; Cliffel, D. E.; Lukehart, C. M. *J. Phys. Chem. B* ***2001***, *105*, 8097-8101.

[28] Tremiliosi-Filho, G.; Kim, H.; Chrzanowski, W.; Wieckowski, A.; Grzybowska, B.; Kulesza; P. *J. Electroanal. Chem.* ***1999***, *467*, 143-156.

[29] Waszczuk, P.; Solla-Gullón, J.; Kim, H-S.; Tong, Y. Y.; Montiel, V.; Aldaz, A.; Wieckowski, A. *J. Catal.* ***2001***, *203*, 1-6.

[30] Tripković, A. V.; Poppvić, K. D.; Grgur, B. N.; Blizanac, B.; Ross, B. N.; Marković, N. M. *Electrochim. Acta* ***2002***, *47*, 3707-3714.

[31] Gökağaç, G.; Kennedy, B. J. *Verlag der Zeitschrift für Naturforschung* ***2002***, *57b*, 193-201.

[32] Abdel Rahim; M. A.; Khalil, M. W.; Hassan; H. B. *J. Appl. Electrochem.* ***2000***, *30*, 1151-1155.

[33] Lima, A.; Coutaneau, C.; Léger, J. - M.; Lamy, C. *J. Appl. Electrochem.* ***2001***, *31*, 379-386.

[34] Shropshire, J. A. *J. Electrochem. Soc.* ***1965***, *11*, 465-469.

[35] Samjeské, G.; Wang, T.; Löffler, T.; Baltruschat, H. *Electrochim. Acta* ***2002***, *47*, 3681-3692.

[36] Wang, Y.; Facini, E. R.; Cruz, G.; Zhu, Y.; Ishikawa, Y.; Colucci, J. A.; Cabrera; C. R. *J. Electrochem. Soc.* ***2001***, *148*, C222-C226.

[37] Horkans, J.; Shafer, M. W. *J. Electrochem. Soc.* ***1977***, *124*, 1196-1202.

[38] Sogimoto, W.; Ohnuma, T.; Murakami, Y.; Takasu, Y. *Electrochem. Solid-State Lett.* ***2001***, *4*, A145-A147.

[39] Wang, B.; Li, X.; Dong, S. *J. Electroanal. Chem.* ***1997***, *435*, 23-30.

[40] Dong, S.; Wang, B. *J. Electroanal. Chem.* ***1994***, *370*, 141-143.

[41] Wang, B.; Li, X.; Dong, S. *J. Electroanal. Chem.* ***1997***, *435*, 23-30.

[42] Lui, S.; Zhang, Q.; Wang, E.; Dong; S. *Electrochem. Commun.* ***1999***,*1*, 365-369.

[43] Ioroi, T.; Fujiwara, N.; Siroma, Z.; Yasuda, K.; Miyazaki, Y. *Electrochem. Commun.* ***2002***, *4*, 442-446.

Chapter 2

Experimental

2.1 The chemicals

All of the chemicals, which were consumed in this work, were used as received without any additional purification. The assay of the active ingredients written on the commercial bottles was recognized when diluted solutions were prepared.

Methanol with a minimum CH_3OH assay of 99.8% was supplied by Merck. The liquid was commercially ranked as an ACS reagent. In all of the experiments that were conducted with methanol, a 1 M CH_3OH aqueous solution was prepared by diluting the 99.8% methanol with the proper amount of de-ionized water.

A 37% formaldehyde solution was received from Produitis Chimiques ACP Chemicals Inc. The assay appearing on the commercial bottle shows 36.5-38.0% HCHO. The formaldehyde has been commercially classified as an ACS grade reagent. A 1 M HCHO aqueous solution was prepared by dilution with de-ionized water.

The nitric acid was purchased from Fisher Scientific. The information on the bottle shows that the acid meets the ACS specifications. The commercial assay reveals 68.0-70.0% of HNO_3, with a maximum amount of dissolved impurities of nearly 20 ppm. The acid was used in this work without any dilution.

Dilute aqueous solutions of sulfuric acid were prepared from the Aristar® acid

(98%) received from BDH Chemicals Ltd. Aqueous H_2SO_4 solutions with different concentrations were prepared by dilution with the proper amounts of de-ionized water.

A 5% by mass Nafion solution was received from Aldrich Chemical Company. The solution was used as received with no further purification. Besides Nafion, 45% of the solution's content is water. The rest of the solution is a mixture of low molecular weight aliphatic alcohols.

Water was distilled by using a conventional distillation system, and de-ionized with a Nanopure II de-ionizer provided by Barnstead. Aqueous MoO_4^{2-} solutions were prepared from $Na_2MoO_4.2H_2O$ (Baker). ACS grade Ammonium heptamolybdate tetrahydrate was received from Aldrich Chemical Company, Inc.

A commercial carbon supported Pt catalyst was purchased from E-tek Inc. Although the accompanying information states that the Pt content of the Pt/C powder is 20%, the gravimetric analysis (section 5.2.1) revealed the presence of ca 18.5% Pt.

Industrial grade N_2 gas was used in this work to purge the aqueous solutions from any dissolved O_2. The nitrogen was supplied by Air Liquide Inc.

2.2 The electrochemical instrumentation

Two types of potentiostats were employed in this work. A Hokuto Denko® HA-301 potentiostat/galvanostat and a HB-104 function generator was used to perform the work described in Chapter 3. A Pine® RDE 4 potentiostat/galvanostat, with an internal function generator, was utilized to conduct the measurements reported in Chapters 4 and 5. These instruments were connected to personal computer interfaces. The

electrochemical data were obtained with the assistance of the CV3 software program written by Colin Cameron.

2.3 The electrochemical cell and the electrodes

All of the voltammetric experiments in this work were performed in a conventional three compartment glass cell. Before each electrochemical run, the cell was washed with the de-ionized water, then it was rinsed with the test solution. With all of the electrochemical measurements that were obtained in this work, a Pt wire and an Ag/AgCl electrode were employed as the auxiliary and the reference electrodes, respectively.

Two kinds of working electrodes were utilized: a Pt disc and a glassy carbon electrode with 0.458 cm^2 and 0.071 cm^2 surface areas, respectively. The bare glassy carbon electrode was modified prior to the utilization, as described in chapters 3 and 5. The working electrodes were mechanically polished with a 0.3-micron alumina aqueous suspension before conducting any electrochemical or surface modification procedures. All of the electrochemical measurements were performed at room temperature.

2.4 The general procedure for potential sweep experiments

The first step in a potential sweep experiment is purging of the test solution inside the cell with N_2 for at least 5 min. Connection of the working, the reference, and the counter electrodes immersed in the test solution to the potentiostat then takes place. After that, the lower and the upper limits of the scan as well as the sweep rate are carefully adjusted to the desired values.

Figure 2.1 is a block diagram that shows connections of the three electrodes to the potentiostat/function generator. In brief, the potential applied between the working and the reference electrodes is varied in a controlled fashion, and the generated current is plotted as a function of the time or the applied potential.

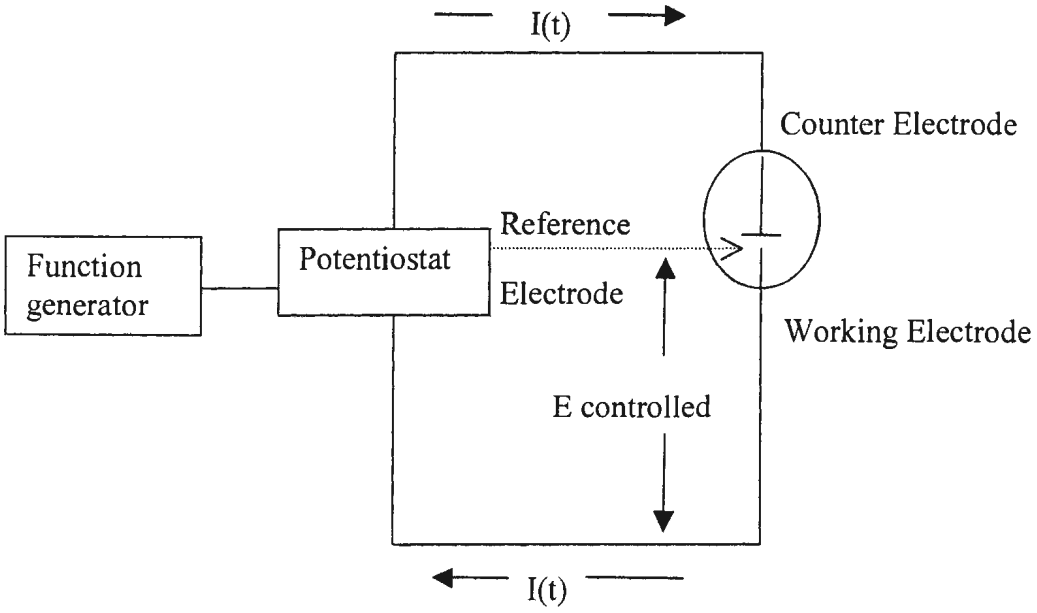

Figure 2.1: Components of the cyclic voltammetric experiment

2.5 Reproducibility

Each voltammeteric measurement was repeated for at least three times. Precision of the measurements can be expressed in terms of the percent relative standard deviation (%RDS), that is defined as the percent ratio of the standard deviation (s) to the mean (x). In terms of equations, the percent is:

$$\%RDS = 100*s/x \qquad (2.1)$$

In general, a %RDS of ca.15.3 was estimated for the electrochemical measurements performed in this work.

Chapter 3

Supported Platinum Ink Type Electrodes

3.1 Introduction

Pt based catalysts are usually employed for the electro-oxidation of molecular hydrogen as well as low molecular weight organic fuels.[1] The oxidation of methanol, ethanol, and formaldehyde has been intensively studied with several kinds of Pt catalysts.[2-4] In general, single crystal and polycrystalline Pt electrodes are employed for the investigation of the mechanism of the oxidation reaction.[5,6] Supported catalysts are usually involved in estimation of the activity of the catalyst toward the oxidation reaction.[7,8] The reduction of oxygen has also been investigated with these different types of Pt catalysts, with similar intensity.[9-11]

In a DMFC, Pt is utilized at both the anode for the oxidation of methanol, and at the cathode for the reduction of molecular oxygen. To make the maximum use of the Pt particles used for the electrolysis, Pt should be dispersed on a support with the highest possible dispersion to provide the ultimate utilization of the precious metal.

Several chemical and electrochemical methods have been employed for the dispersion of Pt on a carbon or a polymer support.[12-14] For fuel cell purposes, carbon supports are usually used since they provide the proton and the electronic connections

required for the consumption of both methanol and O_2, as it is illustrated in equations 3.1 and 3.2:

$$CH_3OH + H_2O \rightleftharpoons CO_2 + 6H^+ + 6e^- \quad (3.1)$$

The protons shown in equation 3.1 penetrate through the catalyst layer to the membrane electrolyte between the anode and the cathode while the electron flow to the cathode through an external circuit. The protons and the electrons meet O_2 at the cathode where the reduction reaction occurs as:

$$O_2 + 4H^+ + 4e^- \rightleftharpoons 2H_2O \quad (3.2)$$

The utilization of bare carbon supports has limitations,[15] since they exhibit significant permeability toward the gases involved in the cathodic and the anodic processes. To reduce the problem of poor proton transport within the carbon supports and, as a consequence, to maximize the utilization of the employed catalyst, carbon supported Pt catalysts are usually mixed with polymer electrolytes such as Nafion®. Nafion is a perfluorosulfonic acid polymer that provides an intimate contact between the catalyst layers, the anode and the cathode, and the membrane electrolyte.[16]

Lee et al[17]studied the effects of Nafion impregnation on the performance of a commercial carbon supported Pt catalyst toward the oxidation of H_2 and the reduction of O_2. They found that the cell potential increases in the presence of the impregnated Nafion. Tracking the impedance behavior of the H_2/O_2 cell exhibited a four-fold decrease in the cell resistance in going from 0 to 0.6 mg/cm^2 Nafion loading. The reported catalytic promotion has been attributed to extension of the reaction zones and the

consequent decrease in the charge transfer and the internal resistance. The added Nafion gave a chance for extra amounts of the reactants to reach the surface of the catalyst.

Willson and Gottesfeld[18] described the perpetration of Nafion-loaded Pt/C catalysts. The first step in the preparation procedure is the mixing of the Pt/C powder with a Nafion solution to form an ink. The prepared ink is then applied to a dry ionomeric membrane sheet by direct painting. Finally, the painted membrane is baked at 160 to 190 °C. The coated membrane is usually known as the membrane electrode assembly (MEA).

Estimation of the performance of a catalyst, within a fuel cell, by conducting experiments with its corresponding MEA demands control of several experimental variables.[19] Besides the catalytic activity of the dispersed catalyst, the efficiency of the cell as a source of power will be highly affected by the temperature, the flow rates of the gases involved in the electrochemical reactions, and the dryness, or the hydration, of the MEA. The inherent catalytic properties of the utilized catalyst may be masked by the effects of these factors. The apparent activity may not reflect the actual efficiency of the catalyst.

As was demonstrated in Chapter 1, a preliminary estimation of the catalytic activity of different pure and alloyed Pt catalysts, toward the oxidation of methanol, has been performed with single working electrodes. Therefore, with the direct application of the catalyst/Nafion ink into the surface of a flat and conductive electrode, possible interference that accompanies the use of an MEA will be eliminated.

Glassy carbon electrodes are well known as conductive, polishable, solvent impermeable, and mechanically stable materials.[20] Modification of glassy carbon

electrodes is usually conveniently achieved due to the presence of a variety of surface functionalities.

A straightforward contact between a glassy carbon electrode and ink has been achieved separately by Schmidt et al[21] and Gojcović and co-workers.[22] Schmidt applied an aqueous suspension of the catalyst into the surface of a previously polished glassy carbon electrode. The catalyst was then left to dry at room temperature. The Nafion solution was then added over the dried catalyst. On the other hand, Gojcović's method, which is also known as the ink method, involves mixing of the Nafion and the catalyst powder by ultrasonication. After formation of homogeneous ink, an aliquot from the suspension is placed onto a glassy carbon surface. The suspension is allowed to dry at room temperature, then the electrode is further heated at 75 °C to complete the drying.

The oxidation of methanol on different carbon supported Pt catalysts have been studied by Gojcović and Vidaković.[23] The electrodes have been prepared by the ink method using Pt on Vulcan XC-72 (Pt/XC-72), Pt on Black Pearls (Pt/BP), and Pt on Shawinigan Acetylene Black (Pt/SAB) commercial catalysts. The oxidation reaction has been found to be slightly dependent on the Pt loading. A flat maximum specific activity has been reported with about 20%Pt/BP. Effects of the type of the commercial carbon on the rate of methanol oxidation showed that the rate measured with Pt/SAB is two to three times faster than on the other carbon supports. The enhancement has been attributed to the high OH coverage of the Pt/SAB. As it was mentioned in Chapter 1, adsorbed hydroxyl groups participate in the oxidative removal of CO_{ads} and hence, promote the catalytic efficiency.

Shan and Pickup employed the ink method to study the Pt utilization and the oxidation of O_2 on a commercial Pt/C catalyst and on home made polymer supported Pt catalysts.[24] The polymer supported catalysts showed lower percentages of Pt utilization. The reported variation has been attributed to several factors: the poor contact between the polymer and the metallic sites, and blockage of the Pt sites with the polymer. However, both of the supported catalysts showed similar oxygen reduction kinetics. Equivalent oxidation currents were reported when the kinetic currents were normalized for the active Pt areas.

Glassy carbon surfaces are usually contaminated during and after the course of the electrolysis, mostly by organic residues or any contaminant that may exist near the electrode surface. These contaminants aggregate at the surface, mainly in the form of an adsorbed layer that depresses the performance of the electrode. Several activation procedures have been employed for the activation of the glassy carbon electrodes. The most common procedures involve mechanical polishing, heat treatment, or electrochemical preactivation.[25]

The purpose of this chapter is firstly to test the reproducibility of the ink method. The second purpose of this chapter is to demonstrate the evaluation of %Pt utilization. Notes about the activation of glassy carbon electrodes will be mentioned within the context of the chapter.

3.2 Experimental

3.2.1 Preparation of the ink

20% Pt/Vulcan XC72 (Etek Inc.) was weighed into a 20 mL scintillation vial and then 5% by mass Nafion® solution in an aqueous mixture of low aliphatic alcohols was added. The ingredients were mixed to provide a metal loading of ca. 4.3 μg/μL. The mixture was stirred overnight to assure the formation of a homogeneous suspension.

3.2.2 Delivery of the ink

To check the reproducibility of the ink delivery, 1 μL portions of the ink were applied to small weighing dishes. The samples were left to dry for about 3 hours and then weighed by using a Chan 27 Electronic Balance®.

3.2.3 Electrode preparation

By means of a micropipette, 1 μL portions of the suspension were applied to the surfaces of 0.071 cm^2 glassy carbon discs that were previously polished with 0.3 micron alumina polishing paste. The coated electrodes were then left to dry overnight.

3.2.4 Electrochemistry

A conventional three electrode glass cell was employed with the modified carbon

disc as the working electrode, a Pt wire counter electrode, and a silver/silver chloride reference electrode (0.197 V vs. RHE). The electrochemical measurements were performed at room temperature using a Hokuto Denko® HA-301 potentiostat/galvanostat and HB-104 function generator. The electrolyte was 0.5 M H_2SO_4 diluted from stock (BDH® Chemicals) with nanopure de-ionized water.

3.2.5 Activation of bare glassy carbon electrodes

In some experiments, the electrochemical pretreatment program employed by Shi and Shiu[26] was applied to activate bare glassy carbon electrodes. In brief, the electrodes were polished with the 0.3 μm alumina suspension. Then, the potential of the electrode was held at 2.0 V vs. Ag/AgCl, for 3 min and after that at –1.0 V, for 0.5 min, in 0.50 M H_2SO_4 solution. Finally, the potential was scanned from – 0.5 to 1.0 V, at 100 mVs^{-1}, and then to – 0.5 V.

3.3 Results

3.3.1 Delivery of the Ink

Figure 3.1 represents masses of the Pt/C samples weighed after vaporization of water and the other volatile components, and after correction for the mass of the Nafion (ca. 46 μg per μL ink). Each sample was weighed twice. The mass of the catalyst varies significantly between samples.

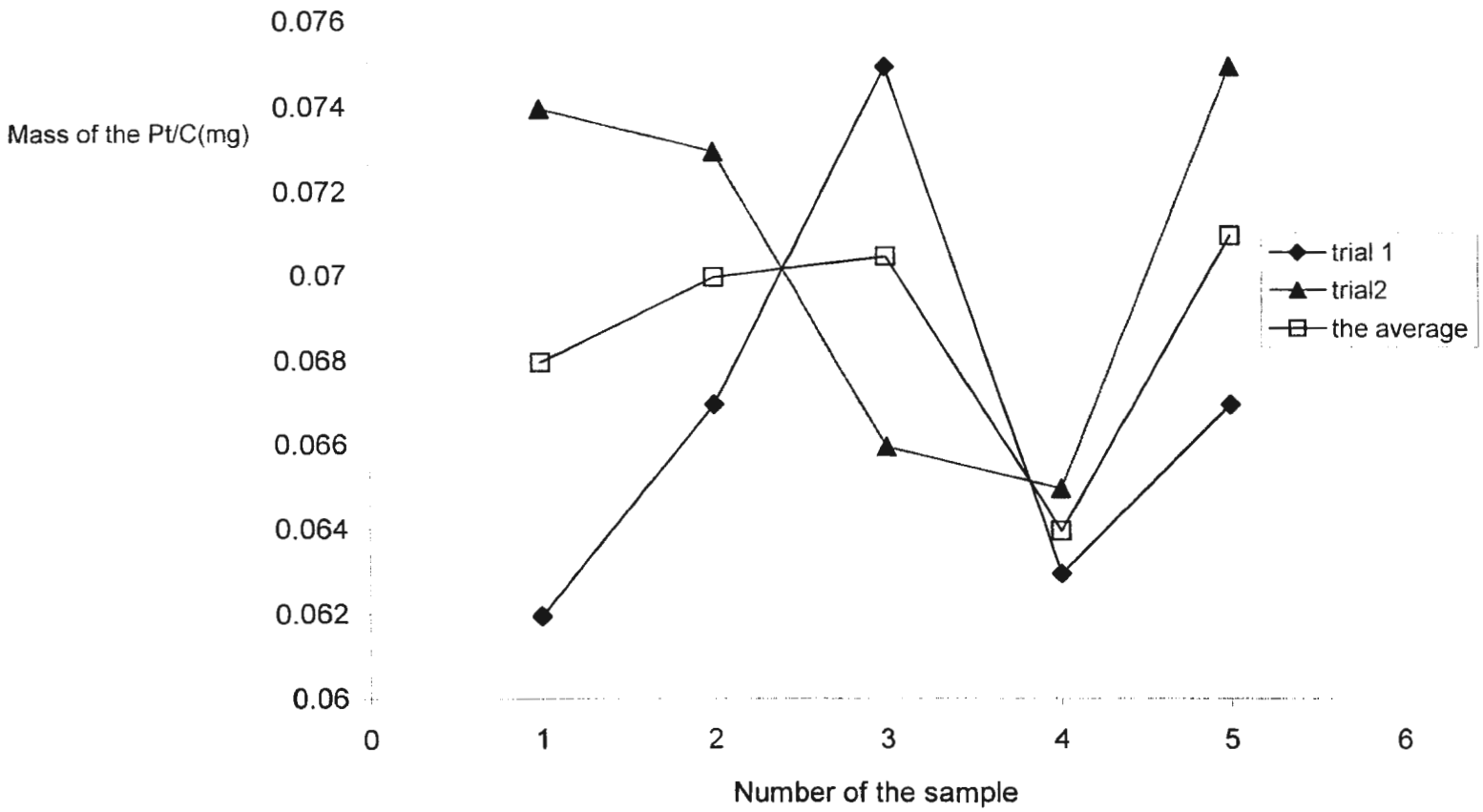

Figure 3.1: Reproducibility in delivery of the ink (the weighed masses were corrected for the mass of the Nafion)

3.3.2 Estimation of the Pt utilization

Cyclic voltammetric features usually observed with polycrystalline platinum surfaces are clear in the cyclic voltammogram of the prepared ink type electrode, as it is shown in figure 3.2. The main features are the hydrogen adsorption/desorption region at around – 0.10 V vs. Ag/AgCl, and the PtO formation/reduction at higher positive potentials.

Due to the high surface areas of platinum dispersed on the carbon supports, charges that accompany hydrogen adsorption/desorption are much greater than those calculated for flat polycrystalline platinum surfaces. Evaluation of the active platinum surface area is therefore very important. The utilization of the Pt catalyst can then be estimated.

The charge under the H-adsorption region in a cyclic voltammogram, Q_H, can be evaluated by integration, as shown in figure 3.3. Q_H is divided by 210 $\mu C/cm^2$, which is the charge generated during the adsorption of a single layer of hydrogen atoms to yield the electrochemically active area.

Platinum utilization can be defined as the ratio of the electrochemically active area to the total area of the electrocatalyst layer. The total area can be calculated from the mean particle size (4 nm dia.), estimated with the assistance of X-ray diffraction analysis,[24] and the mass of the dispersed Pt particles. Figure 3.4 represents %Pt utilizations calculated for two 20%Pt/Vulcan carbon electrodes prepared by the ink method. Utilizations obtained throughout this work were 100% within experimental uncertainty.

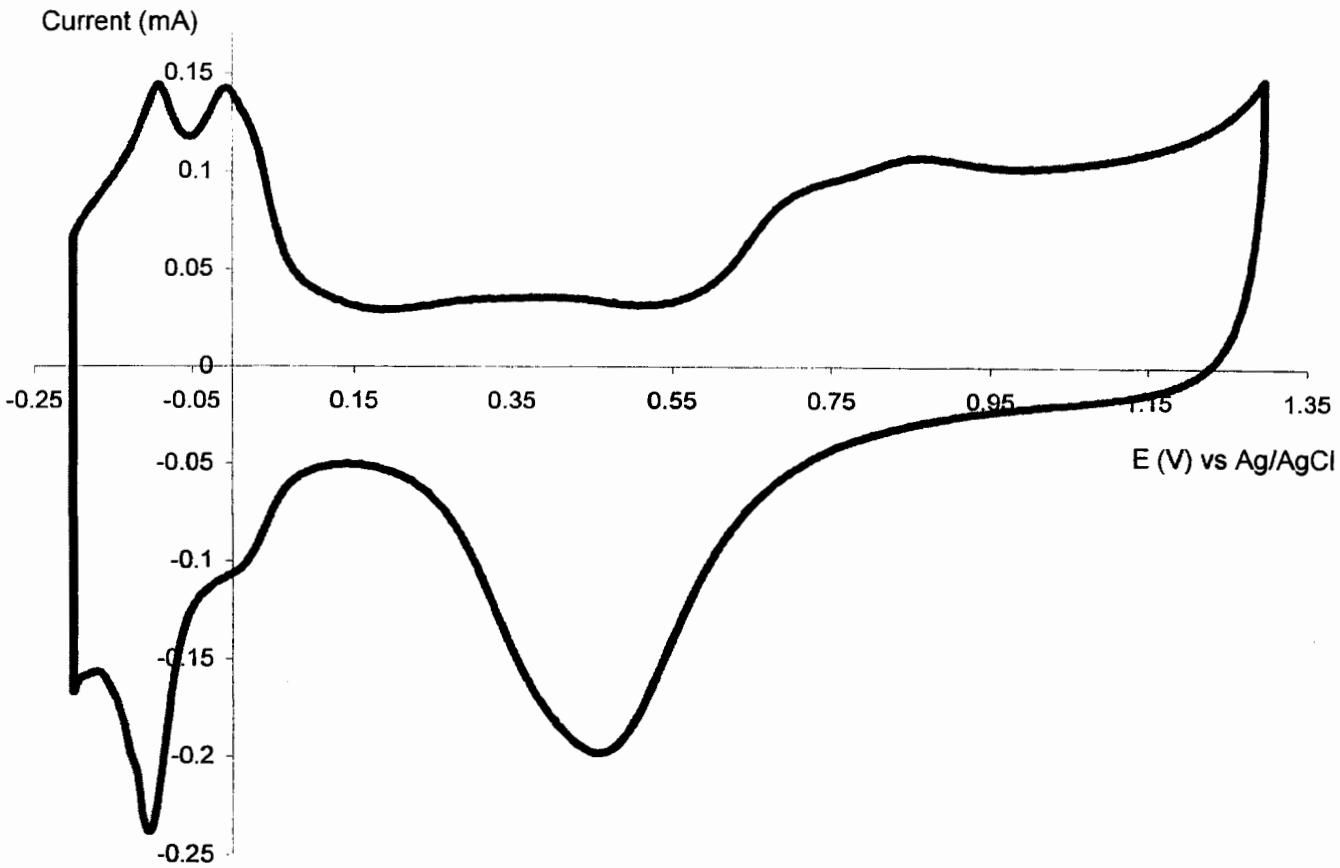

Figure 3.2: Cyclic voltammogram of the commercial catalyst in 0.5M H_2SO_4.
Scan rate = 100 mVs^{-1}

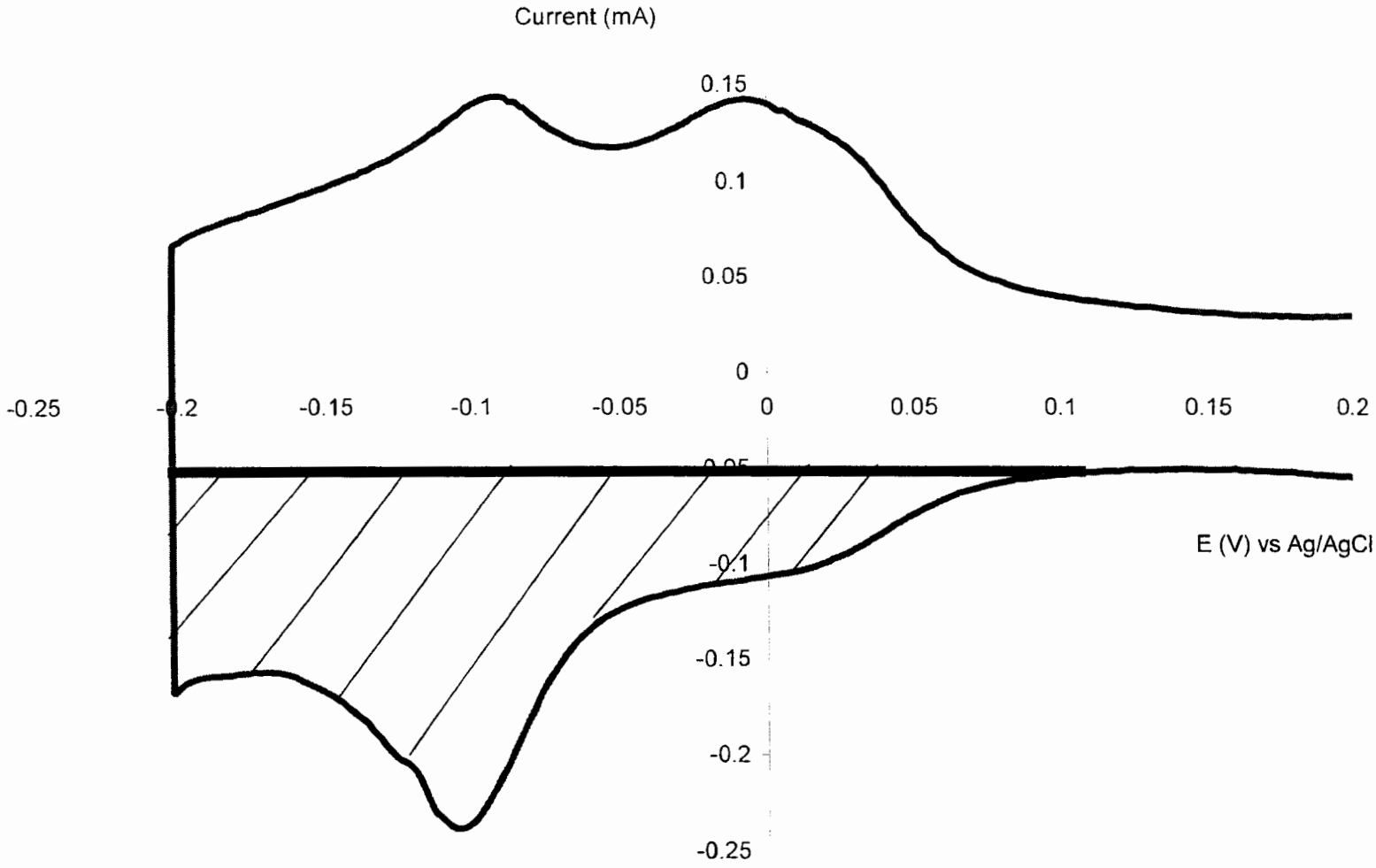

Figure 3.3: The hydrogen adsorption region (the dashed area only)

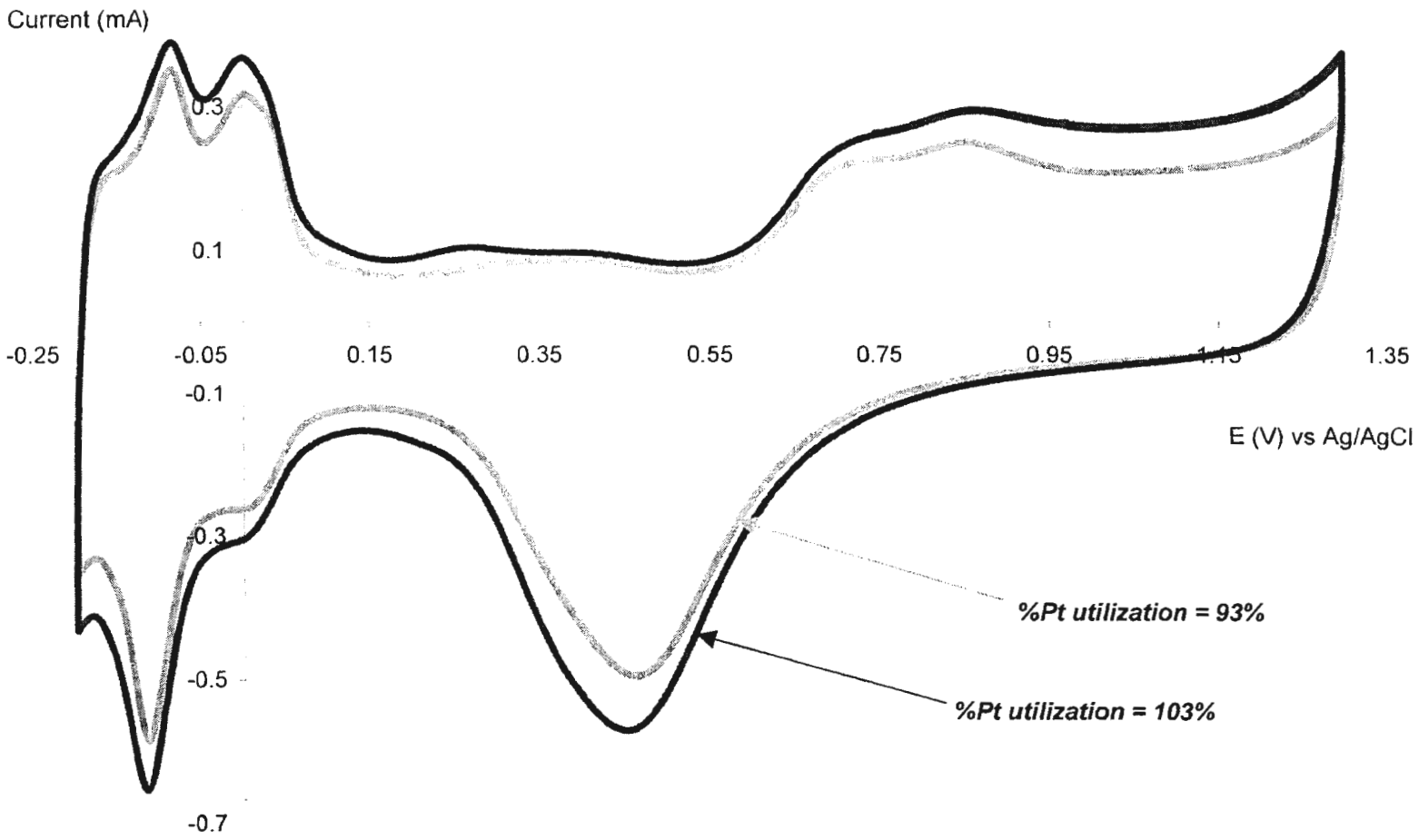

Figure 3.4: Cyclic voltammograms of two commercial Pt/C electrodes, prepared by the ink method, in 0.5M H_2SO_4. Scan rate = 100 mVs^{-1}

3.3.3 Effect of the electrochemical pretreatment

In an attempt to investigate the effect of the pretreatment on the efficiency of the glassy carbon electrodes, the method employed by Shi and Shiu[26] was followed for activation purposes. The effect of the activation is shown in figure 3.5. A comparison between cyclic voltammograms of the electrode before and after the activation showed that the current increased by several orders of magnitude. Figure 3.6 compares the electrochemical behavior of the activated electrode before and after the coating with the 20% Pt-Etek. The electrochemical features of the glassy disc masked those of the coated electrode, especially in the double layer region.

3.4 Discussion

3.4.1 Reliability of the ink method

The precision of analytical data can be defined as the extent of the mutual agreement among data obtained under identical experimental conditions. The precision in the measurements shown in figure 3.1 was attributed to the even distribution of the Pt/C particles in the ink suspension. Although, the measured masses of the Pt/C samples are much higher than the expected value. The mass of the delivered Pt/C dose should be ca. 21 μg, which contains ca. 4.3 μg of Pt. The average of the measured Pt/C samples, shown in figure 3.1, is close to 70 μg, indicating the presence of another component besides the Pt and the carbon support. The additional mass was attributed to the hydration of the

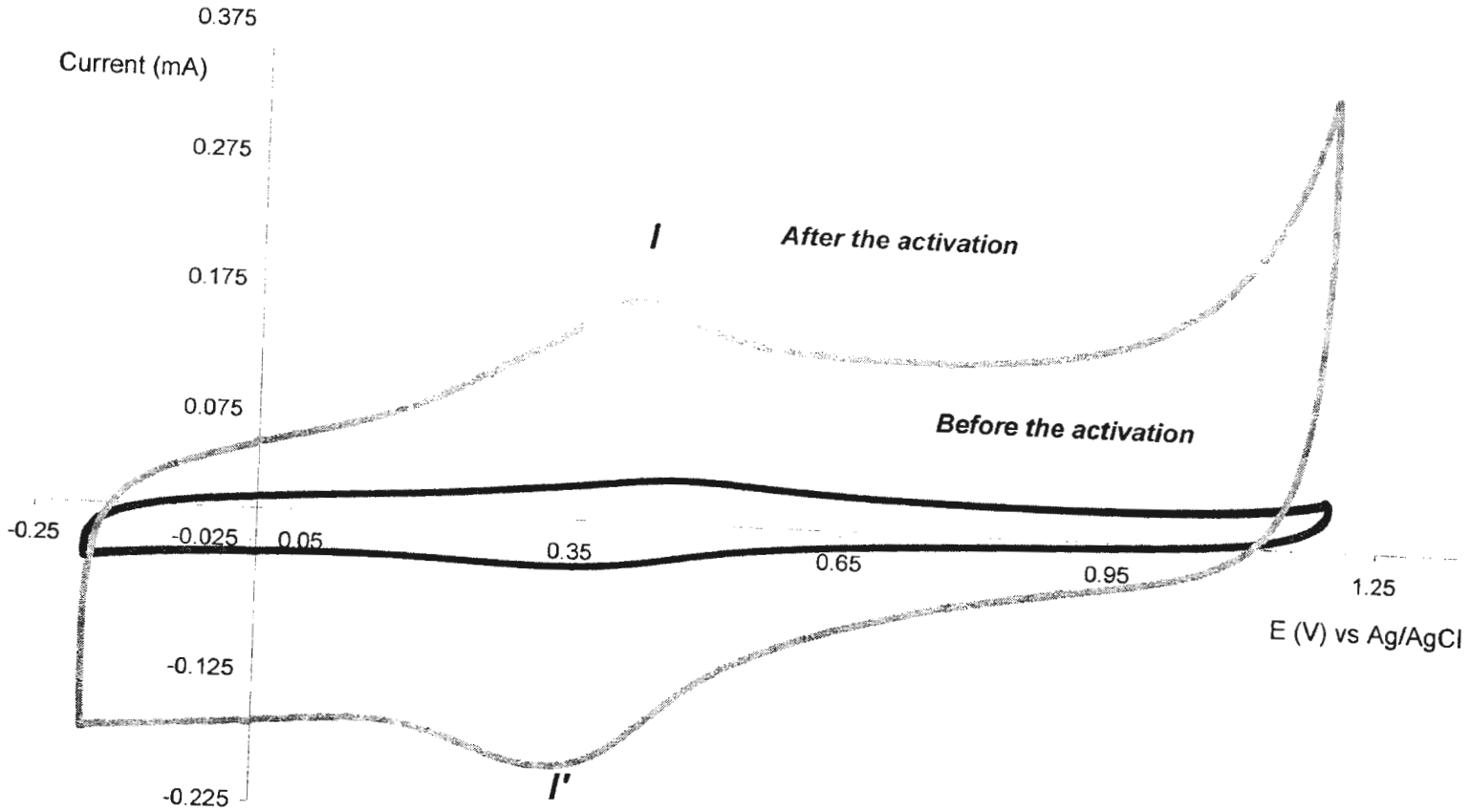

Figure 3.5: Effect of the electrochemical pretreatment on cyclic voltammetry of glassy carbon electrodes in 0.5M H_2SO_4. Scan rate = 100 mVs^{-1}

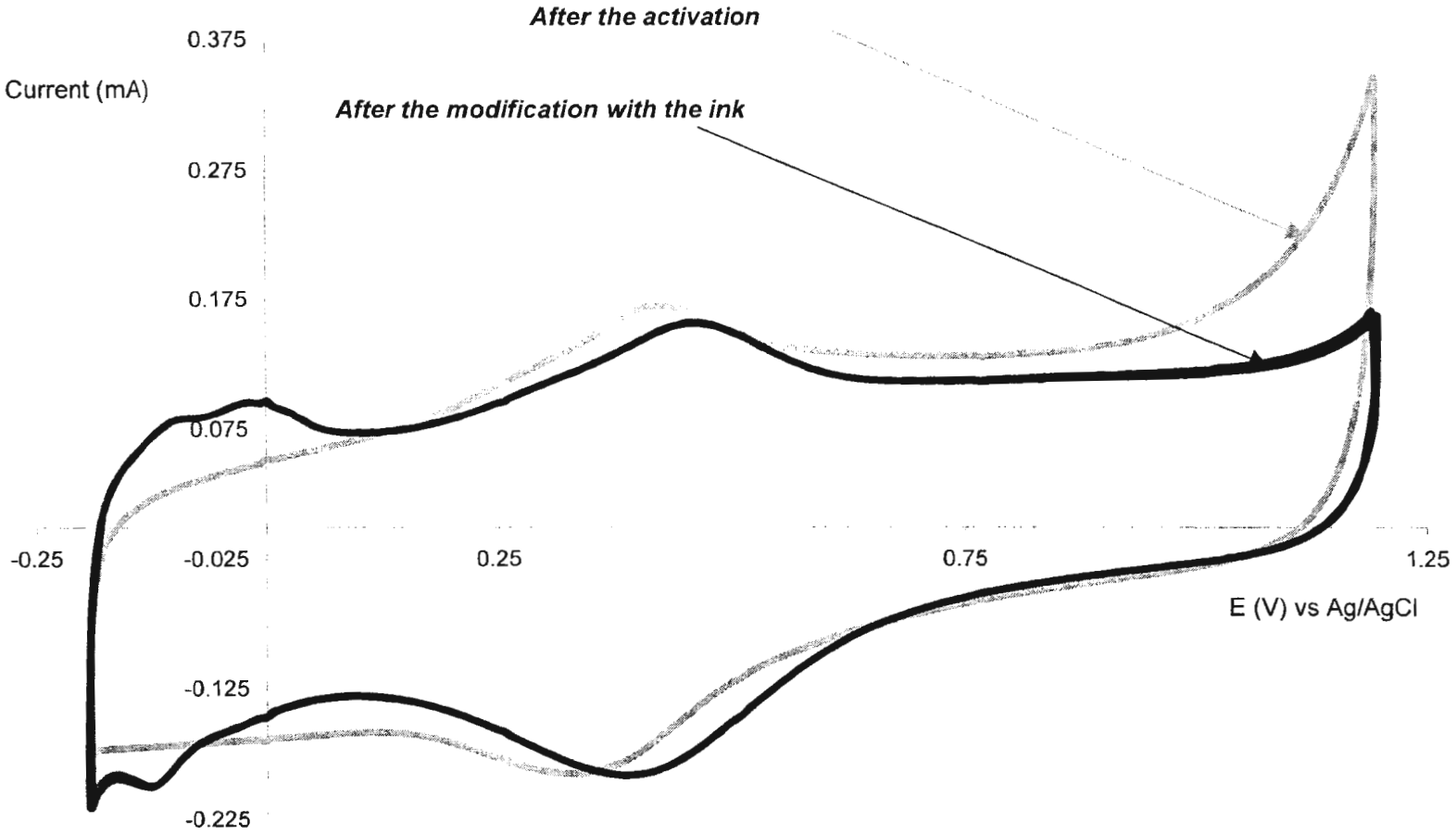

Figure 3.6: Cyclic voltammograms of a glassy carbon electrode, before and after the modification with the ink, in 0.5M H_2SO_4. Scan rate = 100 mVs^{-1}

Nafion and/or the retention of the other solvents, due to insufficient drying of the samples.

The results shown in figure 3.4 support this conclusion. The calculated %Pt utilizations are close to 100%, indicating the delivery of a Pt loading of ca. 60 μg/cm^2, or in other words, the delivery of 4.3 μg Pt, in agreement with the value that was obtained on a theoretical basis. Indeed, with the application of 70 μg Pt/C, which corresponds to ca. 14 μg Pt, the estimated %Pt utilization should exceed 300%. The %Pt utilizations shown in figure 3.4 supports the proposal that the extra mass is due to the presence of the hydrated Nafion and/or retained solvents.

3.4.2 The electrochemical pretreatment

The increase in the current shown in figure 3.5, after the electrochemical pretreatment has been attributed to the electrochemical activity of the quinone/hydroquinone redox couple, especially the redox couple I/I' shown in the figure. Cycling the potential of the bare glassy carbon electrodes in acidic solution has been found to be accompanied with the growth of a transparent, hydrous, porous, and non-conductive thin film on the surface of the activated electrode.[27] The surface redox waves have been reported and attributed to the surface bound quinones as well as surface phenolic and carboxylic hydroxyl groups.

Almost all of the electrochemical features of Pt are absent from the cyclic voltammogram shown in figure 3.6. Only portions of the H-adsorption/desorption region appear at potentials more negative than 0 V. The rest of the voltammogram represents the

electrochemical behavior of the surface quinones and the hydroxyl groups that were observed before the application of the ink. The voltammogram shown in figure 3.2 was obtained with a Pt/C coated glassy carbon electrode that has been only polished with an alumina suspension. It was found that this simple mechanical polishing does not mask the electrochemical properties of the applied catalyst, and so is preferred.

3.5 Conclusion

Direct application of supported platinum catalysts to conductive surfaces facilitates investigation of their catalytic activities. Almost all of the interference that was noticed with the MEA characterization can be removed. Reliability of the ink methodology as a way of providing approximately equal doses of the ink was demonstrated by the ink delivery experiment. Electrodes prepared by the ink method showed excellent stability and durability.

For the investigation of the electrochemical properties of a certain catalyst, with the utilization of the ink method, a simple polishing with an alumina suspension is preferred over an electrochemical activation program. An electrochemical pretreatment of a bare glassy carbon electrode would be helpful in other studies when the electrochemical reaction of interest occurs on the surface of the bare electrode, with the absence of any further modification.[28,29]

List of references

[1] Steele, B. C. H.; Heinzel, A. *Nature* ***2001***, *414*, 345-352.

[2] Tripković, A. V.; Marinković, N.; Popović, K. Dj.; Adžić, R. R. *R. J. Electrochem.* ***1995***, *31*, 993-1003.

[3] Oliveira Neto, A.; Giz, M. J.; Perez, J.; Ticianelli, E. A.; Gonzalez, E. R. *J. Electrochem. Soc.* ***2002***, *149*, A272-A279.

[4] Olivi, P.; Bulhões, L.O. S.; Léger, J.-M.; Hahn, F.; Baden, B.; Lamy, C. *J. Electroanal. Chem.* ***1994***, *370*, 241-249.

[5] Herrero, E.; Franaszczuk, K.; Wieckowski, A. *J. Phys. Chem.* ***1994***, *98*, 5074-5083.

[6] Li, W. S.; Tian, L. P.; Huang, Q. M.; Li, H.; Chen, H.Y.; Lian, X. P. *J. Power Sources* ***2002***, *104*, 281-288.

[7] Gloaguen, F.; Léger, J.-M.; Lamy, C. *J. Appl. Electrochem.* ***1997***, *27*, 1052-1060.

[8] Bouzek, K.; Mangold, K.-M.; Jüttner, K. *J. Appl. Electrochem.* ***2001***, *31*, 501-507.

[9] Giacomini, M. T.; Ticianelli, E. A.; McBreen, J ; Balasubramanian, M. *J. Electrochem. Soc.* ***2001***, *148*, A323-A326.

[10] Neergat, M; Shukla, A. K; Gandhi, K. S. *J. Appl. Electrochem.* ***2001***, *31*, 373-378.

[11] Genies, L.; Faure, R.; Durand, R. *Electrochim. Acta* ***1999***, *44*, 1317-1329.

[12] Ioroi, T.; Fujiwara, N.; Siroma, Z.; Yasuda, K.; Miyazaki, Y.; *Electrochem. Commun.* ***2002***, *4*, 442-446.

[13] Lima, A.; Coutaneau, C.; Léger, J.-M.; Lamy, C. *J. Appl. Electrochem.* ***2001***, *31*, 379-386.

[14] Zhang, H.; Wang, Y.; Fachini, E. R.; Cabrera, C. R. *Electrochem. Solid-State. Lett.* ***1999***, *2*, 437-439.

[15] Jia, N.; Martin, R. B.; Lefebvre, M. C.; Pickup, P. *Electrochim. Acta* ***2001***, *46*, 2863-2869.

[16] Wilson, M. S.; Valerio, J. A.; Gottesfeld, S. *Electrochim. Acta* ***1995***, *40*, 355-363.

[17] Lee, S. J.; Mukerjee, S.; McBreen, J.; Rho, Y. W.; Kho, Y. T.; Lee, T. H. *Electrochim. Acta* ***1998***, *43*, 3693-3701.

[18] Wilson, M. S.; Gottesfeld, S. *J. Electroanal. Chem.* ***1992***, *139*, L28-L30.

[19] Gloaguen, F.; Andolfatto, F.; Durand, R.; Ozil, P. *J. Appl. Electrochem.* ***1994***, *24*, 863-869.

[20] Mcreery, R. L. In *Interfacial Electrochemistry: Theory, Experiments, and applications;* Wieckowski, A., Ed; Marcell Dekker, NewYork, ***1999*** p. 631.

[21] Schmidt, T. J.; Gasteiger, H. A.; Stab, G. D.; Urban, P. M.; Kolb, D. M.; Behm, R. J. *J. Electrochem. Soc.* ***1998***, *145*, 2354-2358.

[22] Gojcović, S. Lj.; Zečević, S. K.; Savinell, R. F.; *J. Electrochem.Soc.* ***1998***, *145*,3713-3720.

[23] Gojcović, S. Lj.; Vidaković, T. R. *Electrochim. Acta* ***2001***, *47*, 633-642.

[24] Shan, J.; Pickup, P. *Electrochim. Acta* ***2000***, *46*, 119-125.

[25] Engstrom, R. C. *Anal. Chem.* ***1982***, *54*, 2310-2314.

[26] Shi, K.; Shiu, K-K. *Anal. Chem.* ***2002***, *74*, 879-885.

[27] McCreery, R. L.; In *Electoanalytical Chemistry;* Bard, A.J., Ed.; Marcell Decker, NewYork, ***1991***; Vol. 13, pp 221-373.

[28] Dong, S.; Wang, B. *J. Electroanal. Chem.* ***1994***, *370*, 141-143.

[29] Sullivan, M. G.; Schnyder, B.; Bärtsch, M.; Alliata, D.; Barbero, C.; Imhof, R.; Kötz, R. *J. Electrochem. Soc.* ***2000***, *147*, 2636-2643.

Chapter 4

Methanol Oxidation at Molybdate-Modified Platinum Surfaces

4.1 Introduction

In all of the examples discussed in Chapter 1, the oxidation of methanol to CO_2 on the various kinds of Pt and Pt alloy catalysts occur with the assistance of metals in their metallic forms. The bi-functional mechanism introduced by Watanabe and Motoo[1] is the main proposal that has been employed to explain the catalytic promotion obtained by the alloying of Pt with the other transition metals. However, surface and bulk analysis of several commercial carbon supported PtRu catalysts, carried out by Rolinson et al,[2] has revealed the presence of a significant amount of H_xRuO_y, in addition to the metal alloy. XRD analysis of the commercial catalysts shows the presence of metal alloy; the hydrous Ru oxide is an amorphous material that is missed by the XRD technique. However, X ray photoelectron spectroscopy (XPS), thermal gravimetric analysis (TGA), and elemental analysis determined by glow discharge mass spectroscopy (GDMS) confirmed the presence of the hydrated Ru oxide, $RuO_2.xH_2O$, on the surface and in the bulk of the tested catalysts.

Rolinson et al attributed the catalytic activity of the commercial PtRu catalysts to the Ru oxide rather than metal alloy. It was proposed that the oxide provides the proton and the electron conductivity required in a DMFC at the anode, as it was shown in equation 3.1. In addition, it was postulated that the oxidative removal of the CO_{ads} occurs with the assistance of the Ru-OH groups inherently existing in the Ru oxide.

Biswas et al[3] prepared graphite based Pt electrodes combined with ferric oxide supported Au particles, or $C/Fe_2O_3/Au/Pt$. The fabricated catalyst were examined for the oxidation of methanol in aqueous NaOH. Cyclic voltammetric experiments showed that the catalyst exhibits a higher catalytic efficiency toward the oxidation of methanol relative to its C/Pt and $C/Fe_2O_3/Pt$ counterparts. The last two catalysts showed comparable oxidation abilities, hence, Biswas et al attributed the catalytic promotion to the oxide supported ultrafine Au particles. It was proposed that the Au particles participate directly in the oxidative removal of CO_{ads} or any carbonaceous intermediate generated during the course of the oxidation reaction.

The oxidation of methanol at a tungsten oxide matrix, decorated with Pt and polynuclear oxocyanoruththenium microcenters has been performed by Kulesza et al.[4] All of the ingredients were electrochemically deposited from their respective solutions on the surface of a bare glassy carbon electrode to obtain a catalyst designated as $WO_3/RuOCNRu/Pt$. Several electrochemical programs were applied for the deposition. The efficiency of the prepared catalyst toward the oxidation of methanol in aqueous H_2SO_4 was evaluated by means of cyclic voltammetry and chronoamperometry. The catalyst showed higher performance toward the oxidation reaction than its WO_3/Pt analog, prepared under identical experimental conditions.

Kulesza et al suggested two explanations for the catalytic promotion observed in the presence of the polynuclear oxoruthenium complex. The catalytic enhancement could be due to the presence of ionic Ru species originating from the polynuclear oxoruthenium, which provide hydroxyl groups or radicals able to participate in the

oxidative removal of CO_{ads}. Alternatively the deposition of the oxoruthenium complex could cause morphological changes within the structure of the WO_3/RuOCNRu/Pt catalyst and enhance the Pt utilization over the WO_3/Pt catalyst. With both explanations, the role of the tungsten oxide was supposed to be providing the catalyst with a proton and electron conducting stable support.

Molybdenum oxides have also attracted significant attention as supports. They have the general formula MoO_x, with $2 \leq x \leq 3$. The crystal structures of MoO_2, MoO_3, and the intermediate oxides Mo_4O_{11} (monoclinic), Mo_4O_{11} (orthorhombic), $Mo_{17}O_{47}$, Mo_5O_{14}, Mo_8O_{23}, and Mo_9O_{26} have been determined by Magneli and Kihlborg.[5] Non-stoicheometric molybdenum oxides with complicated structures have also been characterized.[6]

A high surface area MoO_3 supported Pt catalyst has been prepared by Hoang-Van and Zegaoui.[7] The catalyst was obtained by the thermal reduction of H_2PtCl_6 previously impregnated into the Mo oxide support. Further reduction of the prepared catalyst with H_2 led to the formation of a hydrogen molybdenum bronze, H_xMoO_3. It has been found tha the x value depends on the duration and on the temperature of the reduction.

The production of Pt microparticles dispersed with a film of molybdenum oxides, MoO_x, $2<x<3$, on a carbon support has been accomplished by Cabrera et al.[8] The codeposition of Pt and Mo was accomplished by cycling the potential of a glassy carbon working electrode in an aqueous H_2SO_4 solution containing their metal ion precursors, H_2PtCl_6 and Na_2MoO_4.

Cyclic voltammograms of the MoO_x supported catalyst in an aqueous H_2SO_4 solution exhibited an additional redox couple at slightly higher potentials than the hydrogen adsorption/desorption features usually observed for Pt surfaces. The extra redox couple has been attributed to the MoO_2/MoO_3 pair.

Cabrera et al[9] prepared a series of catalysts, with different Pt/Mo ratios, using the electrodeposition method mentioned above. These Pt/Mo oxide catalysts were employed for methanol oxidation in acidic aqueous solutions. Cyclic voltammmetry of the catalysts in CH_3OH/H_2SO_4 solution exhibited two oxidation peaks. The more positive peak was proportional to the square root of the scan rate, hence, it was attributed to the oxidation of methanol that is brought to the surface by diffusion. The less positive peak was found to be proportional to the scan rate, indicating a voltammetric response from an adsorbed species, namely the carbonaceous residues produced from methanol decomposition. At constant Pt(IV) concentration in the deposition solution, it was found that the maximum catalytic effect toward methanol oxidation occurs with the electrochemical deposition from 0.3 M MoO_4^{2-}, while at constant MoO_4^{2-}, the maximum effect occurs with deposition from 3.0 mM Pt(IV).

To account for the catalytic effect of the prepared Pt/Mo oxides on the oxidation of methanol, the mechanism represented by equations 4.1 to 4.4 has been postulated:

$$5\ Pt + CH_3OH \rightleftharpoons Pt\text{-}CO + 4\ Pt\text{–}H \qquad (4.1)$$

$$Pt + MoO_x + H_2O \rightleftharpoons MoO_x\text{–}OH + Pt\text{–}H \qquad (4.2)$$

$$5\ Pt\text{–}H \rightleftharpoons 5Pt + 5\ H^+ + 5\ e^- \qquad (4.3)$$

$$Pt\text{–}CO + MoO_x\text{–}OH \rightleftharpoons CO_2 + H^+ + Pt + MoO_x + e^- \qquad (4.4)$$

The total reaction can be written as:

$$CH_3OH + H_2O \rightleftharpoons CO_2 + 6\,H^+ + 6e^- \qquad (4.5)$$

The electrochemical oxidation of methanol on Pt black, in H_2SO_4 aqueous solution has been studied by Shropshire.[10] Tafel plots of the oxidation reaction showed that it proceeds with high overpotentials. Even when low current densities were withdrawn from the system, overvoltages of several hundreds of millivolts should be applied. This behavior has been attributed to the strong adsorption of methanol molecules at the Pt surface.

Shropshire observed that by the addition of MoO_4^{2-}, to the Pt black surface before the addition of methanol, the oxidation of methanol proceeds readily by the application of overvoltages close to the thermodynamically calculated value. Relatively high current densities were extracted at lower overpotentials, with a significant deviation from the expected Tafel behavior. At high overpotentials, the Pt black modified surface behaves in a manner similar to that of the unmodified surface. This behavior has been attributed to the removal of the adsorbed molybdate layer at high overvoltages, which is followed by strong adsorption of the organic fuel at the electrode surface.

To account for the catalytic effect observed in the presence of MoO_4^{2-}, on the oxidation of methanol on Pt black in H_2SO_4 aqueous solution, a two-step mechanism has been proposed, as shown in equations 4.6 and 4.7. The first step is the chemical reaction between methanol and adsorbed molybdate as:

$$6\,(Mo^{6+})_{ads} + CH_3OH + H_2O \rightleftharpoons 6\,(Mo^{5+})_{ads} + CO_2 + 6H^+ \qquad (4.6)$$

Then, the electrochemical regeneration of $(Mo^{6+})_{ads}$ occurs as:

$$(Mo^{5+})_{ads} \rightleftharpoons (Mo^{6+})_{ads} + e^- \quad (4.7)$$

Shropshire speculated that molybdates occupied less than half of the Pt surface.

The generated ion shown in equation 4.7 undergoes further electrochemical reduction, as shown in equation 4.6, the net result is a magnification of the current produced from the mentioned methanol oxidation reaction.

Li et al[11] studied modification of a polycrystalline Pt surface with molybdate and the oxidation of methanol at the modified surface. It was found that the reduction of MoO_4^{2-} to an adsorbed hydrogen molybdenum (IV) oxide occurs at negative potentials as:

$$MoO_4^{2-} + 4H^+ + 2\,e^- \rightleftharpoons (H_2MoO_3)_{ads} + H_2O \quad (4.8)$$

At higher positive potentials, the reduced molybdate is oxidized to several forms of hydrogen molybdenum bronzes (H_xMoO_3, $0<x<2$). Methanol oxidation at the molybdate modified Pt occurs at potentials lower than those required with the unmodified surface. Greatly enhanced oxidation currents have been reported.

To account for the decreased overpotentials and the enhanced currents, formation of $(H_{1.5}MoO_3)_{ads}$ and $(HMoO_3)_{ads}$ has been proposed. These oxides abstract protons from the adsorbed organic residues produced by methanol decomposition and convert them into CO_{ads} species. The process can be described by equations 4.9 – 4.14:

$$(CH_3OH)_{ads} + 8\,(H_{1.5}MoO_3)_{ads} \rightleftharpoons CO_{ads} + 8\,(H_2MoO_3)_{ads} \quad (4.9)$$

hydrogen molybdenum (IV) oxide is oxidized to regenerate the adsorbed oxide as:

$$(H_2MoO_3)_{ads} \rightleftharpoons (H_{1.5}MoO_3)_{ads} + 0.5\,H^+ + 0.5\,e^- \quad (4.10)$$

For $(HMoO_3)_{ads}$ the cycle occurs as:

$$(CH_3OH)_{ads} + 4\,(HMoO_3)_{ads} \rightleftharpoons CO_{ads} + 4\,(H_2MoO_3)_{ads} \quad (4.11)$$

$$(H_2MoO_3)_{ads} \rightleftharpoons (HMoO_3)_{ads} + H^+ + e^- \quad (4.12)$$

The adsorbed oxides also activate water to act as an oxygen donor to CO_{ads}, on its way to CO_2:

$$CO_{ads} + 4\,(H_{1.5}MoO_3)_{ads} + H_2O \rightleftharpoons CO_2 + 4\,(H_2MoO_3)_{ads} \quad (4.13)$$

and

$$CO_{ads} + 2\,(HMoO_3)_{ads} + H_2O \rightleftharpoons CO_2 + 2\,(H_2MoO3)_{ads} \quad (4.14)$$

These equations show that the presence of the $(H_{1.5}MoO_3)_{ads}/(H_2MoO_3)_{ads}$ and the $(HMoO_3)_{ads}/(H_2MoO_3)_{ads}$ couples assist in keeping the Pt surface clean, and in converting the adsorbed oxidation residues to CO_2.

In this chapter, some of the experiments carried out by Li's group were repeated to verify the activity of Mo bronze modified Pt for methanol oxidation. Additional electrochemical experiments were done for further investigation of the nature of methanol oxidation at a Mo modified Pt electrode surface.

4.2 Experimental

4.2.1 The reagents

Sodium molybdate oxide dihydrate, $Na_2MoO_4.2H_2O$ was purchased from J. T. Baker Co. 99.9% Methanol was supplied from Fisher Scientific, and stock sulfuric acid from BDH® Chemicals. All of the ingredients were diluted to the desired concentrations with nanopure de-ionized water.

4.2.2 Electrochemistry

Cyclic and linear scan voltammetries were carried out using an RDE 4 Pine potentiostat from Pine Instrument Company. The working electrode was a Pt disc (area = 0.458 cm^2), the reference electrode was Ag/AgCl. A Pt wire was employed as a counter electrode.

4.3 Results

A cyclic voltammogram of the Pt electrode used in this work, in aqueous H_2SO_4 solution, is shown in figure 4.1. The curve a shows the current generated by cycling the potential of the working electrode in aqueous H_2SO_4 solution. For comparison purposes, the cyclic voltammogram reported by Li et al[11] under similar conditions is also shown, as curve b. The two voltammograms have the same electrochemical features, although the current density in curve b is greater by a factor of 4 than that of curve a. Since the data in figure 4.1 were normalized for the geometrical area of the electrodes, it can be concluded that Li's electrode was about 4 times rougher than ours.

The presence of molybdate, MoO_4^{2-}, added to the solution causes dramatic changes in the electrochemical behavior at the Pt electrode. Curves a and b in figure 4.2 represent linear scan voltammograms of the Pt electrode in H_2SO_4 and MoO_4^{2-}/H_2SO_4 aqueous solutions, respectively. In the absence of the molybdate, hydrogen desorption occurs from the lower limit of the scan to potentials close to 0.2 V. Pt oxide formation takes place at higher positive potentials. These two processes are considered as the

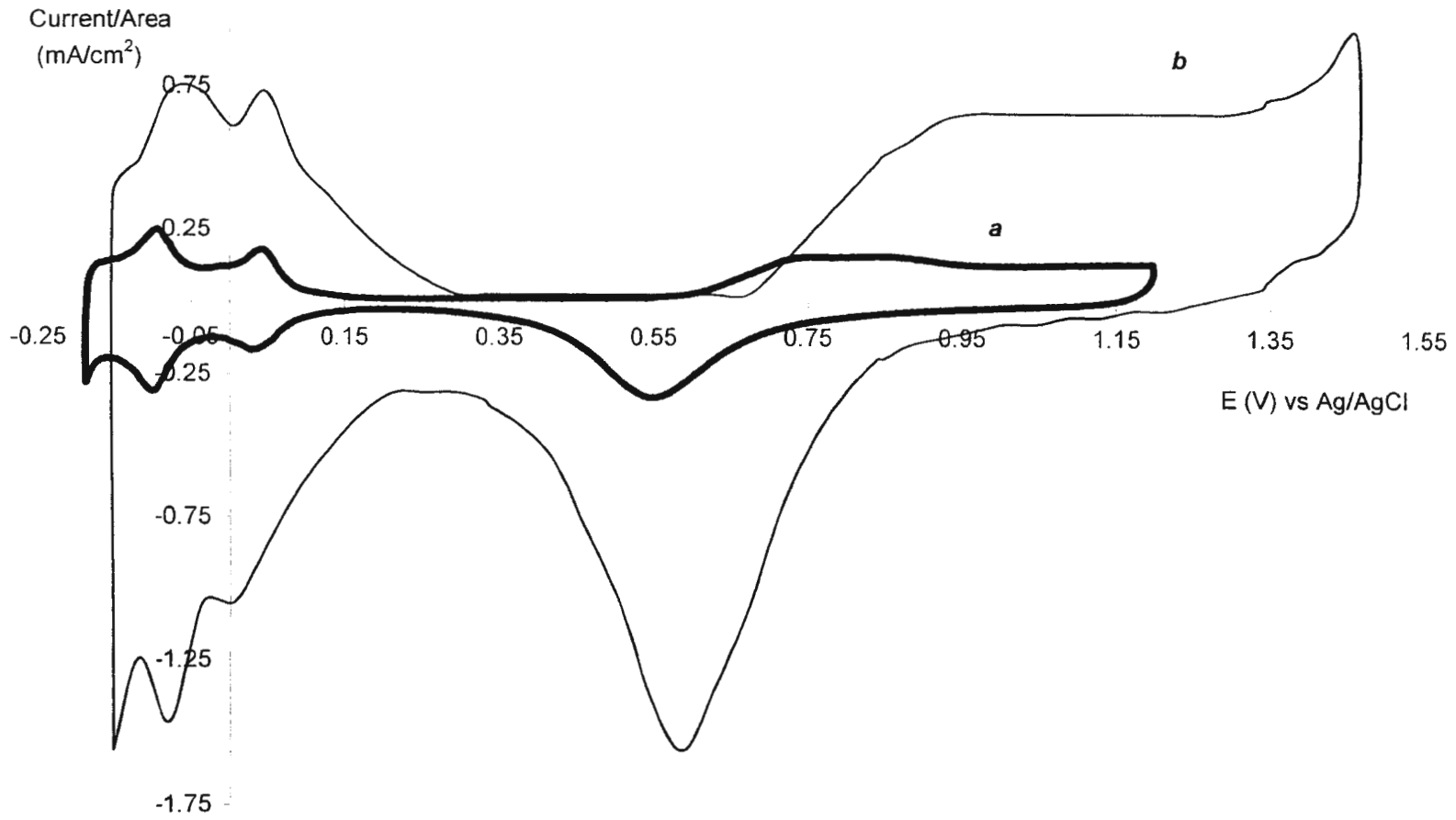

Figure 4.1: Cyclic voltammogram of Pt electrodes in 3.7M H_2SO_4. Scan rate = 100 mVs^{-1}
(a) this work (b) ref. 11

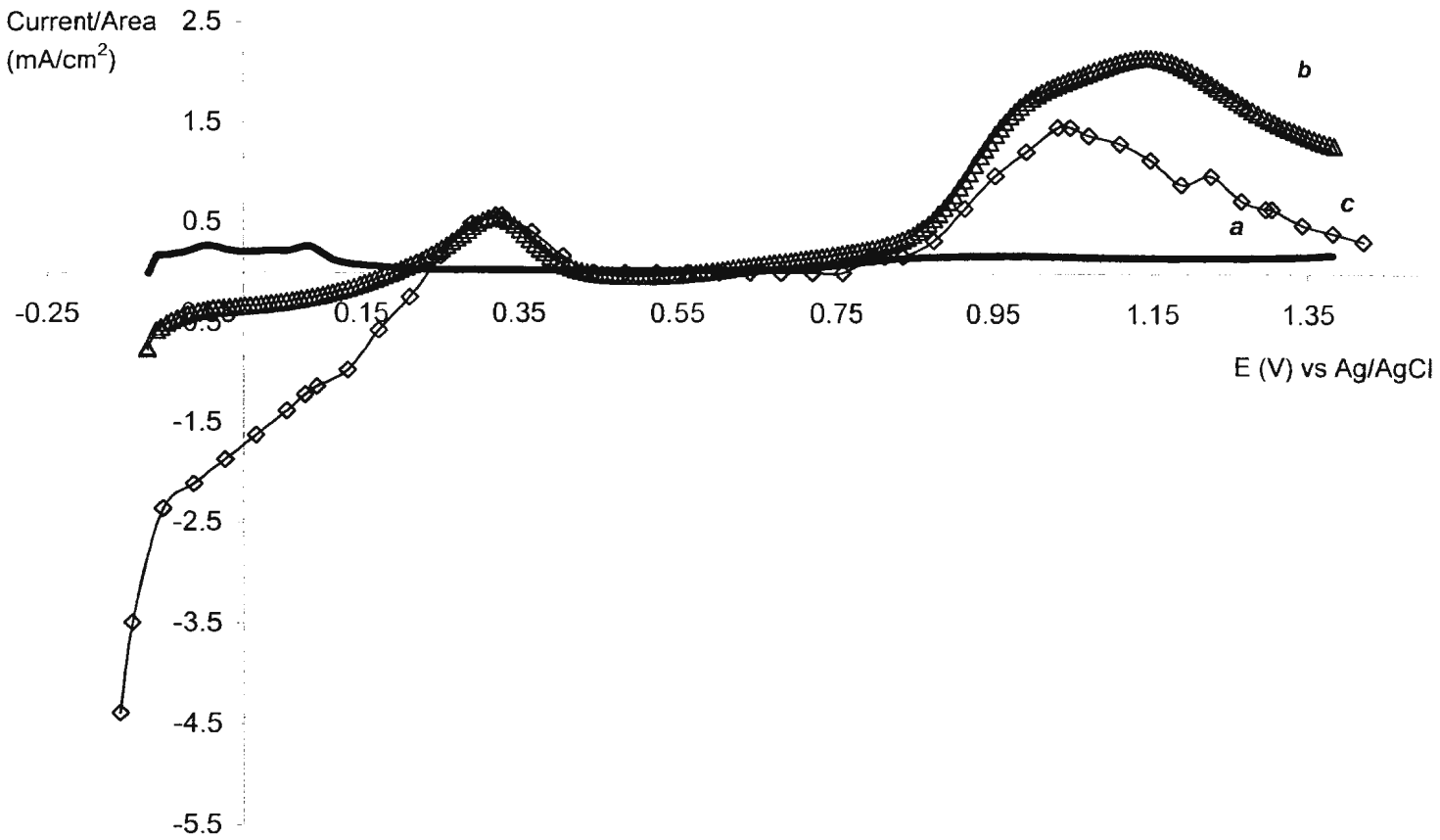

Figure 4.2: Linear scan voltammograms of a Pt electrode in (a) 3.7M H_2SO_4 (b) 0.05M Na_2MoO_4/3.7M H_2SO_4 (c) as (b) but obtained from ref. 11. Scan rate = 100 mVs^{-1}

fingerprints that are universally observed in voltammograms of Pt electrodes in acidic media.

The effect of the molybdate, MoO_4^{2-}, is clear from beginning of the scan, as shown in curve b, figure 4.2. The initially cathodic current decreases as the potential of the working electrode is swept in the positive direction, and the first anodic peak is seen at about 0.30 V (Peak 1). The current then decreases between 0.30 and 0.50 V and then increases to a second maximum (Peak 2) at about 1.20 V. The current decreases after the second peak until the end of the scan.

Curve c in figure 4.2 represents Li's result in MoO_4^{2-}/H_2SO_4. The main difference between curves b and c in figure 4.2 is the current density. Higher current densities were generated by the electrode used by Li, especially near the initial potential and at the two designated peaks.

It was found that holding the Pt electrode at the initial potential of –0.16 V before scanning affects the linear scan voltammogram in MoO_4^{2-}/H_2SO_4. Figure 4.3 shows the scan as a function of time at the initial potential. The first significant change is the variation in value of the current generated at the lower potential limit of the scan, the current at that potential is inversely proportional to the time delay. The peak at 0.30 V (Peak 1) is time independent, with all of the scans exhibiting the same current density at that potential. The current density at the second maximum, at 1.20 V, increases with time up to 1 min, and then it decreases as the initial time delay increases.

The oxidation of methanol on a Pt surface, in aqueous H_2SO_4, is shown in figure 4.4. Curve a is the first scan of a polished Pt disc in CH_3OH/H_2SO_4. It shows little current

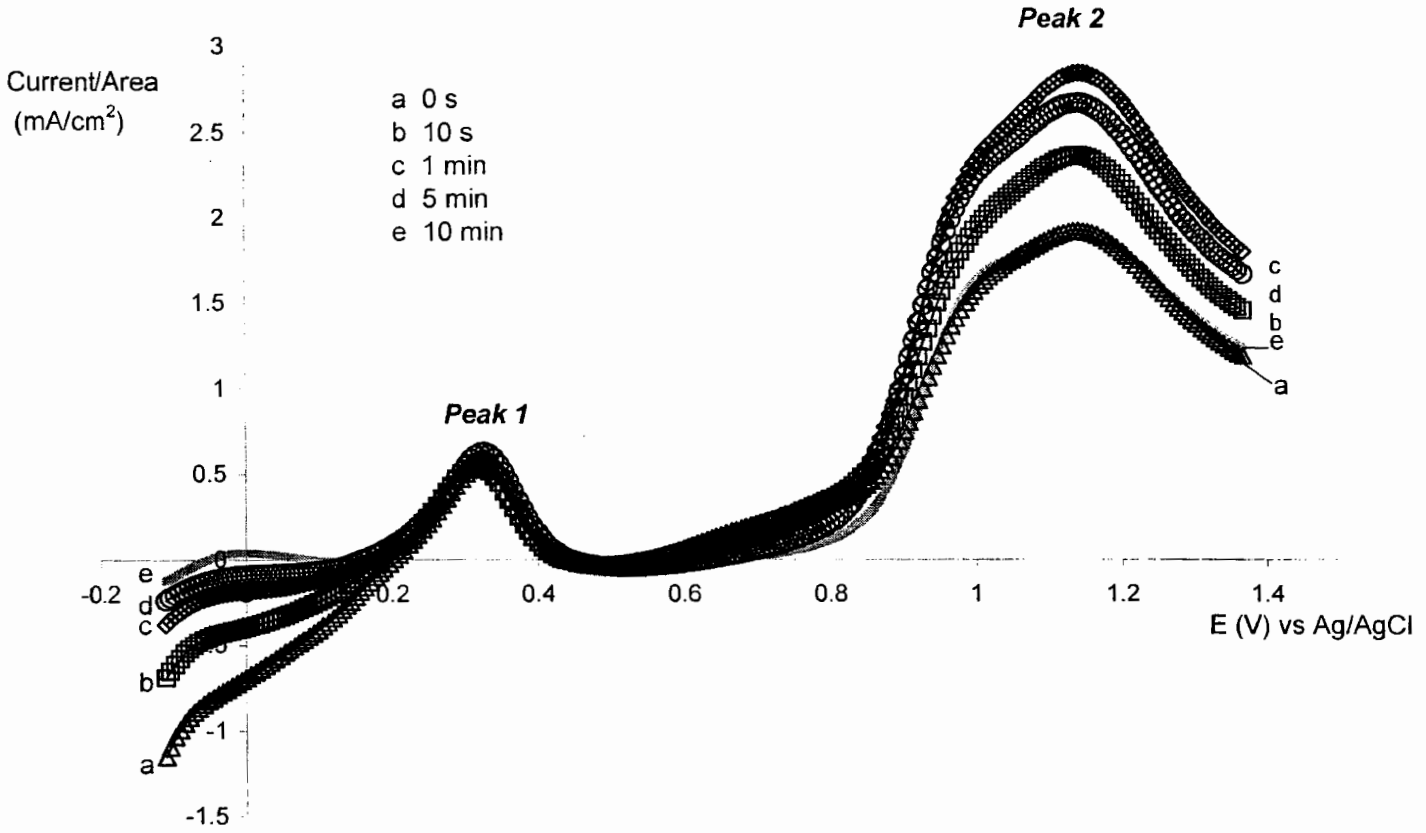

Figure 4.3: Effect of the time at the initial potential on linear scan voltammetry of a Pt electrode in 0.05M Na_2MoO_4/3.7M H_2SO_4. Scan rate = 100 mVs^{-1}

over a wide range of potentials; significant currents were generated only at potentials above 1 V. Curve b represents currents produced during the fifth scan. Further scans gave superimposable curves. Curve c is the corresponding result reported by Li et al, which is quite similar to curve b, especially at potentials above 0.6 V. The two curves exhibit a maximum at ca. 0.75 V, after that, the current decreases until ca. 1 V, and then it increases at higher potentials.

Oxidation of methanol on Pt in the presence of MoO_4^{2-} is entirely different from the results shown in figure 4.4, where methanol was oxidized in the absence of the molybdate. Figure 4.5 is a comparison between the two oxidation processes. It is clear that the onset of oxidation of methanol at the modified Pt surface occurs earlier by about 0.20 V. The oxidation starts at 0.40 V while in the absence of MoO_4^{2-}, little current is observed at that potential.

In the presence of MoO_4^{2-}. as shown in curve b, figure 4.5, the current declines after the peak until ca 0.8 V, then it increases until the end of the scan. In the absence of molybdate, the current reaches a maximum at 0.75 V, then it decreases as the scan proceeds until 1.0 V. The current increases again above 1.0 V with an extent less than that observed at the modified surface.

Similar affects of molybdate on the oxidation of methanol on Pt were reported by Li et al. Figure 4.6 shows the results of that group, curve a, together with the result for the Pt disc used in this work (curve b) in $MoO_4^{2-}/CH_3OH/H_2SO_4$ solution. The main difference between the two curves is the current density; higher current densities were generated by the Pt electrode used by Li et al.

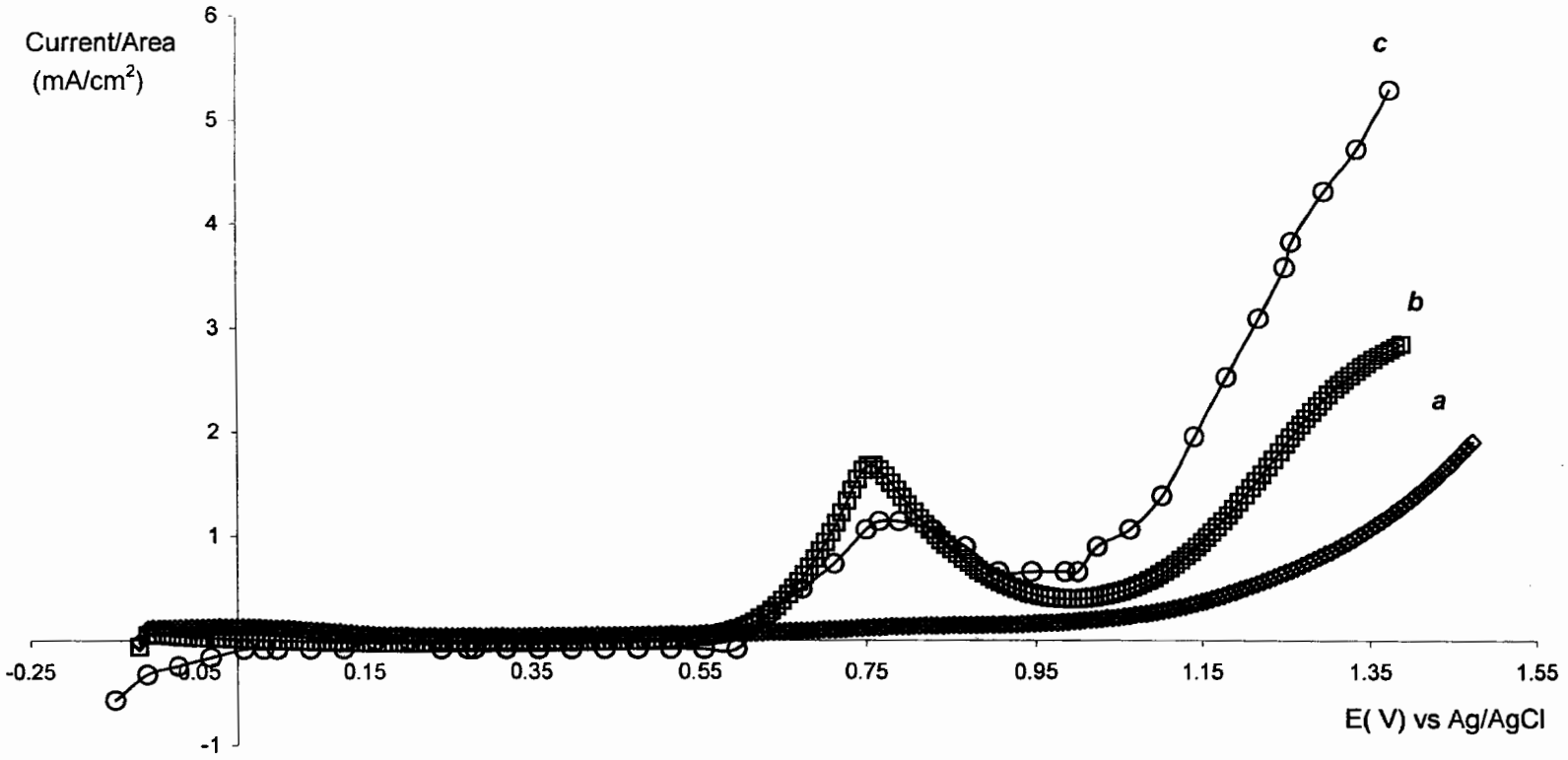

Figure 4.4: Linear scan voltammograms of a Pt electrode in 1M CH_3OH/3.7M H_2SO_4. (a) the first scan (b) the fifth scan (c) from ref. 11. Scan rate = 100 mVs^{-1}

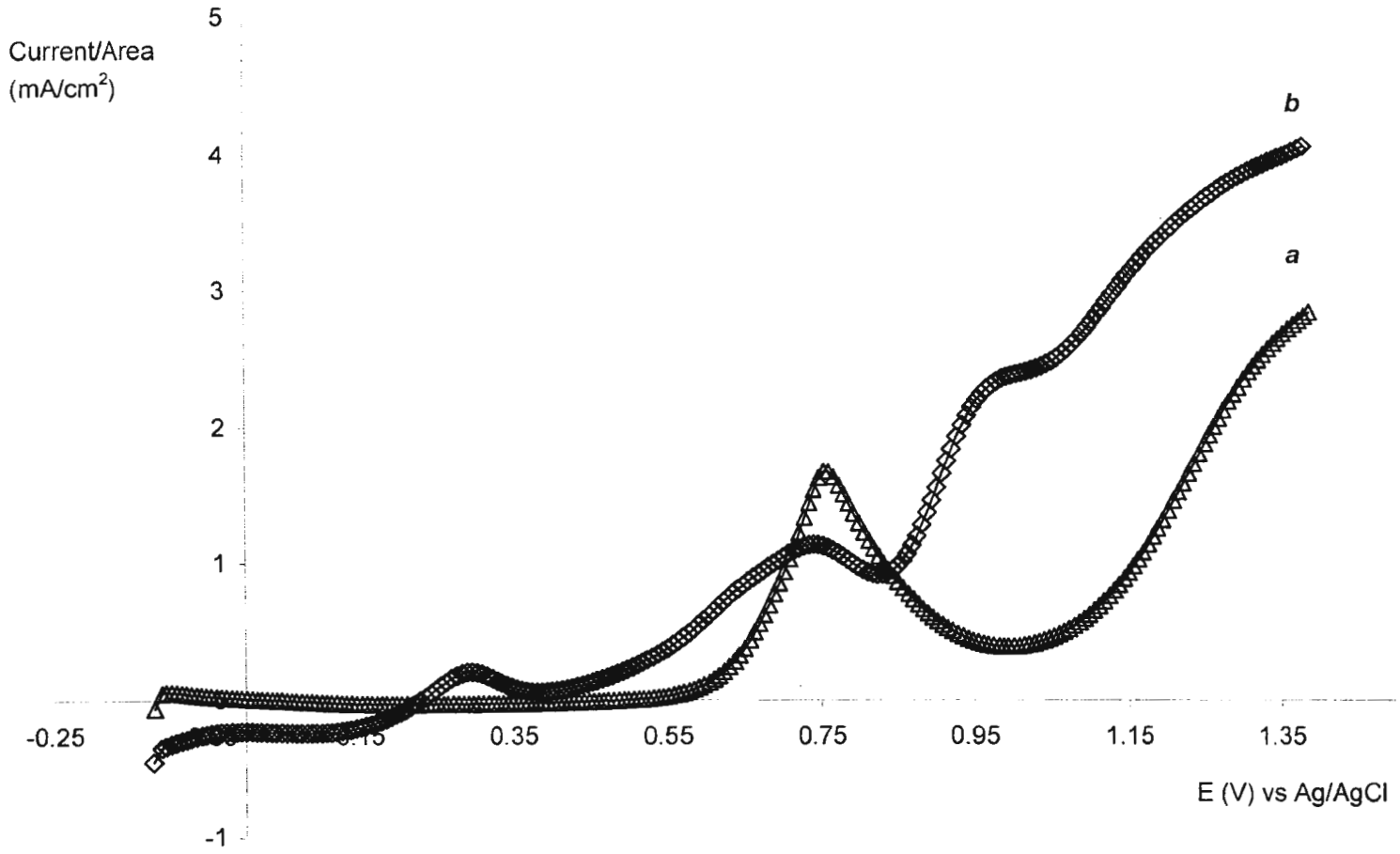

Figure 4.5: Linear scan voltammograms of a Pt electrode in (a) 1M CH_3OH/3.7M H_2SO_4 (b) 0.05M Na_2MoO_4/1M CH_3OH/3.7M H_2SO_4. Scan rate = 100 mVs^{-1}

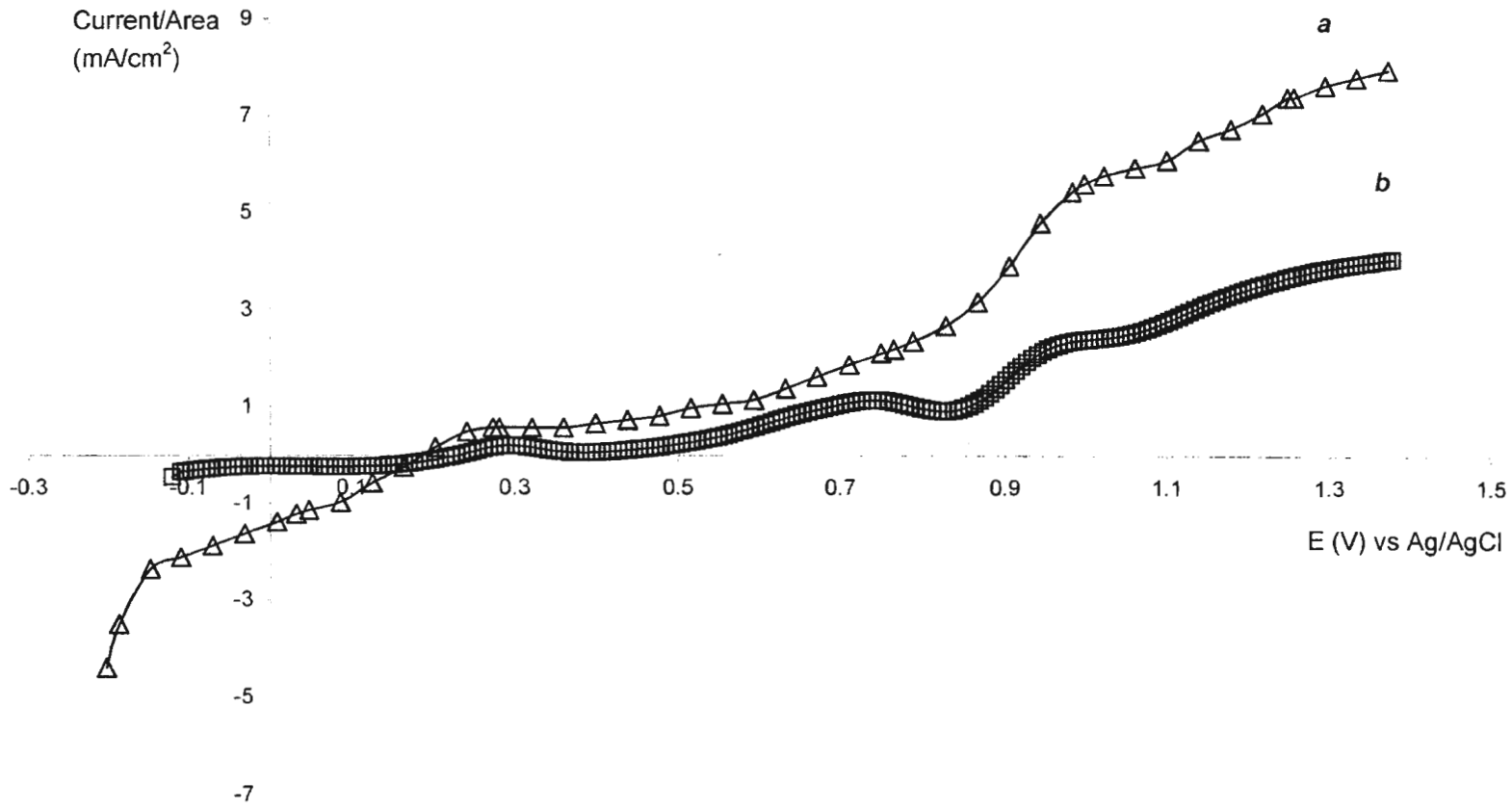

Figure 4.6: Linear scan voltammograms of a Pt electrode in 0.05M Na_2MoO_4/1M CH_3OH/3.7M H_2SO_4. Scan rate = 100 mVs^{-1}. (a) ref. 11 (b) this work

It was also found that the oxidation of methanol at Pt in the presence of MoO_4^{2-} is dependent on the lower potential limit of the scan. Figure 4.7 shows that the highest methanol oxidation currents are generated when the initial potential is below 0.28 V vs. Ag/AgCl. Setting the lower scan limit at more positive values is accompanied by a gradual decrease in the current over all the scan range.

4.4 Discussion

4.4.1 Cyclic voltammetry of Pt in H_2SO_4

The difference in current generated by the electrode used in this work, and that employed by Li et al[11] (as shown in figure 4.1), can be attributed to the difference in the roughness factor value. The roughness factor of an electrode is the ratio between its electrochemically active area and its geometrical area. The electrochemically active areas of the mentioned electrodes were evaluated, as described in Chapter 3 (section 3.2).

H–adsorption/desorption and PtO formation/reduction occur at the electrode's surface as it is universally accepted, therefore one can easily concluded that these processes depend on the electrochemically active area of the electrode, and hence, on its roughness factor. Roughness factors of 2 and 10 were estimated for the electrode used in this work, and that used by Li et al, respectively. This difference accounts for the variation in currents.

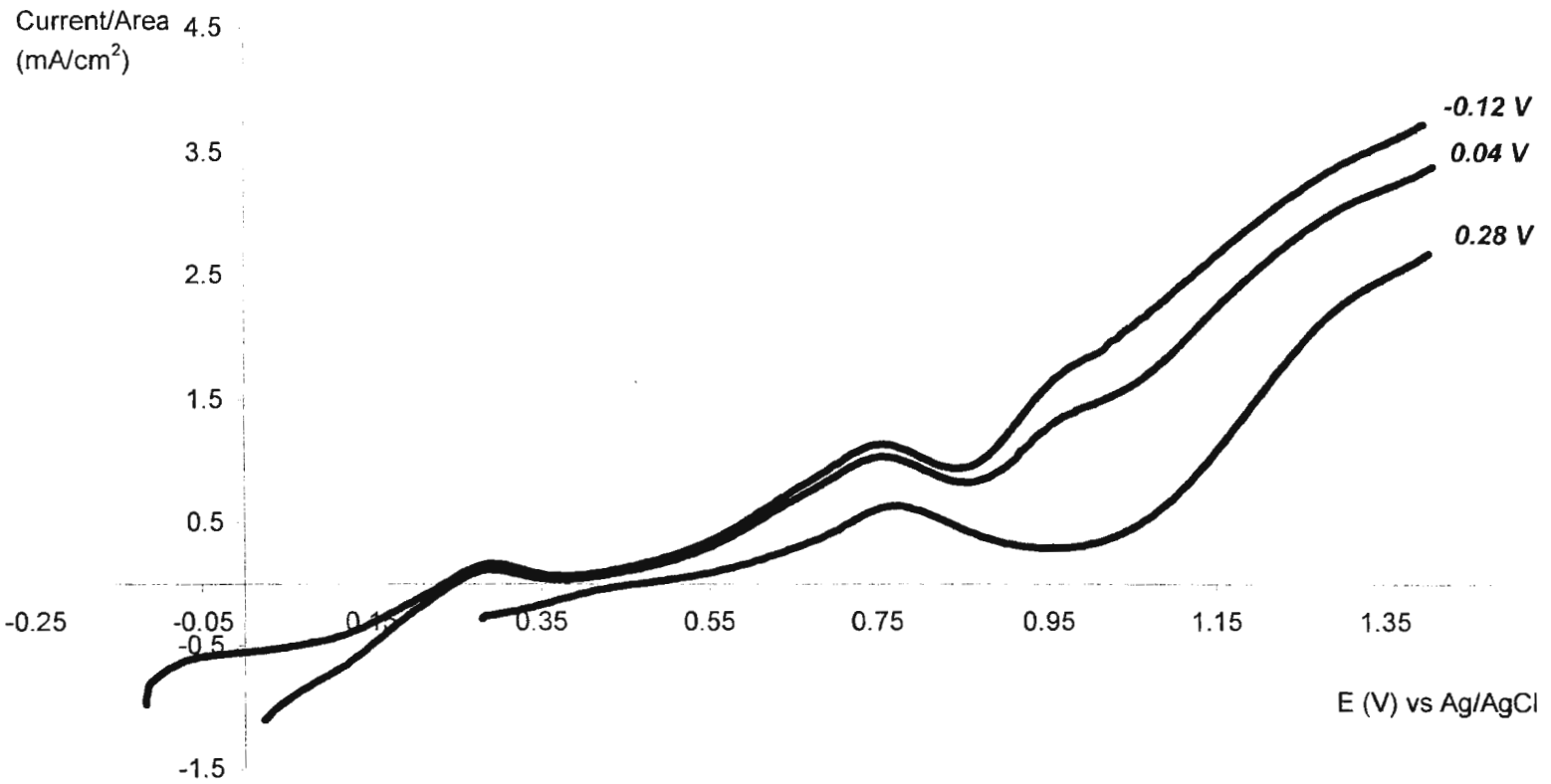

Figure 4.7: Effect of initial potential on linear scan voltammograms of a Pt disc in 0.05 M Na_2MoO_4/1M CH_3OH/3.7M H_2SO_4. Scan rate = 100 mVs^{-1}

A close look at figure 4.1 shows that the two electrodes have equal currents from 0.3 V to 0.6 V. No electrochemical activity is usually observed in this potential range, that is known as the double–layer region. The current in the double–layer area, the double layer current, is directly proportional to the electrode's surface area.[12]

The current reported by Li between 0.3 V and 0.6 V should be 4 times greater than that observed by us, in the same potential range. The unexpected current suppression could be due to the presence of residual atmospheric oxygen. O_2 is usually removed by purging the solution under investigation with an inert gas such as N_2, prior to the electrochemical measurement, as it was described in Chapter 2.

4.4.2 The electrochemical behavior of Pt in MoO_4^{2-}/H_2SO_4 solution.

All of the features observed in the linear scan voltammogram of Pt in H_2SO_4 solution disappear in the presence of MoO_4^{2-}, as shown in figure 4.2. The anodic H-desorption current is replaced by a cathodic current. Holding the potential of the Pt electrode at the lower limit in MoO_4^{2-}/H_2SO_4 causes a green color to develop on surface of the disc. Among the hydrogen molybdenum bronzes produced from the reduction of MoO_4^{2-} in acidic solutions, only H_2MoO_3 has that green color.[11] It can therefore be concluded that at potentials close to the lower limit of the scan, an adsorbed layer of H_2MoO_3 is produced as:

$$MoO_4^{2-} + 4H^+ + 2e^- \rightleftharpoons (H_2MoO_3)_{ads} + H_2O \qquad (4.15)$$

The adsorbed molybdtae is oxidized at higher positive potentials, and two new peaks (Peak 1, and Peak 2 in curve b, figure 4.3) appear at about 0.3 V and 1.2 V as a

consequence of the oxidation process. The latter peak, Peak 2, has higher current densities that may be due to the simultaneous formation of PtO. In general, production of the molybdenum oxides can be formulated as:

$$(H_2MoO_3)_{ads} \rightleftharpoons (H_{(2-x)}MoO_3)_{ads} + x\ H^+ + x\ e^- \qquad (4.16)$$

Curve c in figure 4.2 represents the results obtained by Li et al,[11] under similar experimental conditions. A comparison between curves b and c shows that higher currents were generated at the Pt electrode employed by that group at potentials more negative than 0.2 V. This is due to the higher roughness factor of their electrode.

It was found that the formation of $(H_2MoO_3)_{ads}$ and its oxidation at higher positive potentials is affected by the time difference between potential application and scanning, as shown in figure 4.3. At the initial potential, the current decreases as the time delay is increased. It has been proven that MoO_4^{2-} is brought to the electrode surface by diffusion. Li et al reported that cyclic voltammetry of a Pt electrode in MoO_4^{2-}/H_2SO_4 with different sweep rates showed that the voltammetric response from the adsorbed hydrogen molybdenum bronze, $(H_2MoO_3)_{ads}$, is directly proportional to the square root of the scan rate. The thickness of the diffusion layer increases during the delay time. This is accompanied with depletion in MoO_4^{2-} concentration near the electrode surface, therefore, the current decreases as a result of that depletion.

In figure 4.3, the current at Peak 1 is unaffected by the time delay mentioned above. The peak at 0.30 V is mostly due to the formation of a strongly adsorbed layer, generated from the oxidation of the bronze, $(H_2MoO_3)_{ads}$. Peak 2 increases with the delay

time up to 1 min, however, longer delay times cause a decrease in current at Peak 2, as shown in figure 4.3.

Experimentally, it was found that for delay times of 5 min or more, the green color developed at the initial potential is replaced by a pale gray layer that is easily observed with the naked eye at the electrode surface. The gray layer may be a non-conductive overlayer that was produced as a consequence of holding the potential at the initial potential for time intervals longer than 1 min. This may account for the depression of the second peak shown in figure 4.3.

4.4.3 Oxidation of methanol on Pt in H_2SO_4 solution

The first scan of the Pt electrode in CH_3OH/H_2SO_4 solution is represented by curve a in figure 4.4. There is no sign of methanol oxidation near 0.75 V vs. Ag/AgCl. A peak around that potential is usually observed in linear scan voltammograms of Pt in CH_3OH/H_2SO_4 solution. Its absence may be due to the presence of contaminants on the electrode surface. Significant current densities are only observed near the end of the scan, and that is due to the direct oxidation of methanol to CO_2.

It was found that by repeating of the scan of the Pt electrode in CH_3OH/H_2SO_4 solution for several times, the peak expected for methanol oxidation appears between 0.60 V and 0.80 V with a peak potential close to 0.75 V. Curve b in figure 4.4 is the fifth scan obtained, which can be considered as the steady state scan since further scanning gives superimposable voltammograms. Besides methanol oxidation, several processes occur simultaneously, mainly oxidation of the organic residues produced from methanol

oxidation, in addition to the formation of PtO, that starts at about 0.70 V and lasts until the end of the scan. Currents generated from these processes also contribute to the peak observed at ca 0.75 V.

The oxidation of methanol on Pt in H_2SO_4 solution has also been carried out by Li et al, and they obtained similar results, as shown by curve c in figure 4.4. Curves b and c diverge at potentials more positive than 0.85 V, where the electrode used in this work generates lower currents until the end of the scan. The peak at 0.75 V reported by Li (curve c, figure 4.4) is smaller than that reported by us, as shown in curve b, at the same potential value. The current shown in curve c should be greater than that at 0.75 V, in curve b. The electrode used by Li et al may have been contaminated. The unexpected current suppression may be due to blocking of the electrode by contaminants, as a consequence, a lower current has been reported.

The Pt electrode employed in this work was activated mechanically, as described in Chapter 2, then its voltammetric response was checked for the impurities before conducting any of the experiments reported in this chapter.

4.4.4 The catalytic effect of MoO_4^{2-} on methanol oxidation

Figure 4.5 shows the effect of MoO_4^{2-} on the oxidation of methanol on Pt, in $MoO_4^{2-}/CH_3OH/H_2SO_4$ solution. Methanol oxidation in the absence and the presence of MoO_4^{2-} is represented by curves a and b, respectively. In the presence of MoO_4^{2-}, methanol oxidation occurs at 0.40 V, as shown by curve b, while in CH_3OH/H_2SO_4 solution, the oxidation reaction occurs later at about 0.60 V, as demonstrated by curve a.

In the presence of MoO_4^{2-}, the adsorbed hydrogen molybdenum bronze, $(H_2MoO_3)_{ads}$ that is generated at the lower limit of the scan, undergoes oxidation at about 0.30 V (i.e.) the first peak in curve b, figure 4.3. The generated oxide interacts with methanol and enhances its oxidation rate.

Curves a and b in figure 4.5 show a peak at 0.75 V. In curve a, the current decreases after the peak until 1.00 V is approached, the decrease is mainly due to the formation of a Pt oxide, then the current increases until the end of the scan where direct oxidation of methanol to CO_2 takes place, as shown in equation 4.5. In curve b, the current decreases after the peak at 0.75 V, it reaches a minimum at 0.85 V. At the minimum, an adsorbed Mo oxide is produced, and it is the interaction of the oxide with methanol that is responsible for the current enhancement observed from 0.85 V to the end of the scan.

Li et al carried out the oxidation of methanol on a molybdate-modified surface, as demonstrated by curve a in figure 4.6. Curve b in this figure is the same to curve b shown in figure 4.5. A comparison between scans a and b shows that a higher current density was produced from the rougher Pt electrode used by Li, especially in the area below 0 V and at potentials more positive than 0.80 V.

Determination of formulae of the oxides generated from the oxidation of $(H_2MoO_3)_{ads,}$ at 0.30 V and 1.20 V (shown in figure 4.3) is beyond the scope of this study. In addition, investigation of the nature of interaction of these oxides with methanol needs further experimental work. In this context, coupling of the electrochemical instrumentation with other techniques maybe useful, especially mass spectrometry and

optical methods such as infrared spectroscopy. This would provide real time monitoring of the species that are generated during the course of the electrochemical reaction.

Another experiment that confirms the catalytic effect of $(H_2MoO_3)_{ads}$ on methanol oxidation at a Pt surface is the dependence of the catalytic current on the initial potential, as shown in figure 4.7. Higher currents were generated when the initial potential was adjusted to potentials negative enough for the generation of $(H_2MoO_3)_{ads}$ (i.e.) < 0.28 V vs. Ag/AgCl. Experimentally, it was observed that the extent of green coloration of the electrode decreases when the initial potential is increased which confirms the role of $(H_2MoO_3)_{ads}$ in methanol oxidation at Pt surface.

4.5 Conclusion

The catalytic effect of the molybdate can be attributed to the formation of an adsorbed $(H_2MoO_3)_{ads}$ layer at potentials more negative than 0.2 V vs. Ag/AgCl. The adsorbed molybdate is oxidized at 0.30 V and 1.20 V to adsorbed hydrogen molybdenum oxides, which in turn interact with methanol and catalyze its oxidation.

At the modified surface, methanol oxidation occurs directly after formation of the first hydrogen molybdenum oxide, at a potential less positive than the corresponding oxidation reaction that took place in the absence of MoO_4^{2-}. A second catalytic effect appears at higher potentials, after formation of the second hydrogen molybdenum oxide. This indicates that the presence of molybdenum containing compound enhances the direct oxidation of methanol to CO_2.

The results demonstrated in this chapter are similar to those obtained by Li et al. Electrochemical features of all of the scans are the same with a difference in the current magnitudes. The higher current densities were generated in Li's work was attributed to the higher roughness factor of their electrode.

Formulae of the adsorbed oxides as well as nature of their interaction with methanol are beyond the scope of this work. Further experiments are required to investigate the details of the oxidation of methanol in the presence of MoO_4^{2-}.

List of references

[1] Watanabe, M.; Motoo, S. *Electroanal.Chem.* ***1975***, *60*, 267-273.

[2] Rolinson, D. R.; Hagans, P. L.; Swider, K. E.; Long, J.W. *Langmuir* ***1999***, *15*, 774-779.

[3] Biswas, P. C.; Nodasaka, Y.; Enyo, M.; Haruta, M. *J. Electroanal. Chem.* ***1995***, *381*, 167-177.

[4] Kulesza, P. J.; Grzybowska, B.; Malik, M. A.; Chojak, M.; Miecznikowski, K. *J. Electroanal. Chem.* ***2001***, *512*, 110-118.

[5] Dieterle, M. *Ph.D. thesis*; Technical University of Berlin, Berlin, ***2001***, P2.

[6] Cotton, F. A.; Wilkinson, G. In *Advanced Inorganic Chemistry, 5th ed.;* John Wiely, New York, ***1987***, P807.

[7] Hoang-Van, C.; Zegaoui, O. *Appl. Catal. A: General* ***1995***, *130*, 89-103.

[8] Zhang, H.; Wang, Y.; Fachini, E. R.; Cabrera, C. R. *Electrochem. Solid-State Lett.* ***1999***, *2*, 437-439.

[9] Wang, Y.; Fachini, E. R.; Cruz, G.; Zhu, Y.; Ishikawa, Y.; Colucci, J. A.; Cabrera, C. R. *J. Electrochem. Soc.* ***2001***, *148*, C222-C226.

[10] Shropshire, J. A. *J. Electrochem. Soc.* ***1965***, *112*, 465-469.

[11] Li, W. S.; Tian, L. P.; Li, H. H.; Chen, H. Y.; Lian, X. P. *J. Power Sources* ***2002***, *104*, 281-288.

[12] Wang, J. In *Analytical Electrochemistry, 2nd ed.*; John Wiely, New York, ***2000***, P 21.

Chapter 5

Molybdenum-Modified Carbon Supported Platinum Electrodes

5.1 Introduction

In Chapter 4, the observed enhancement in the current density obtained after the modification of the polycrystalline Pt electrode with MoO_4^{2-}, relative to its unmodified analog, was only ca. 2 mA/cm^2. In addition, the effect of the modification on the oxidation current was observed only at higher positive potentials, mainly between 1 and 1.4 V (look figure 4.5 for example), making the molybdenum modification studied in Chapter 4 valid only for scientific studies, rather than for the desired commercial purposes. The Mo modified Pt electrode provides insufficient current densities for practical applications.

To obtain useful oxidation rates, for DMFC purposes, the anode should sustain current densities higher than 400 mV/cm^2 at potentials lower than 0.3 V vs. RHE.[1] The work in this chapter was therefore aimed at preparing high surface area MoO_x modified catalyst and evaluating them in ink electrodes.

The ink method reported by Schmidt (Chapter 3) has been employed for the preparation of several carbon supported PtMo electrodes for the anodic oxidation of pure and CO-contaminated H_2 mixtures in proton exchange membrane fuel cell (PEMFC) systems.[2,3] Mukerjee et al found that the efficiency of a commercial 4:1 Pt:Mo ink type

electrode,[2] toward the oxidation of H_2/CO mixtures, is higher than that of the state of the art PtRu counterpart. The Mo modified electrode showed a 2 to 3-fold enhancement of CO tolerance. Hydrodynamic and cyclic voltammeteric experiments conducted with a PEMFC revealed that the oxidation of CO_{ads} begins at 0.1 V. The reported catalytic promotion has been explained in terms of the bi-functional mechanism; the Mo provides oxygenated adsorbed species that activate the oxidative removal of the CO adsorbed on the neighboring Pt sites. Facile adsorption and further oxidation of H_2 then occur at the bare Pt sites with the continuous oxidation of the CO_{ads}.

Ioroi et al[3] synthesized a carbon supported Pt/MoO_x catalyst in a stepwise fashion. The mixed-valent MoO_x has been deposited on the carbon support by the chemical reduction of $MoCl_5$, Pt has then been dispersed on the purified MoO_x/C by the thermal decomposition of $Pt(NO_2)_2(NH_3)_2$, previously impregnated into the Mo modified carbon support. An ink from the catalyst has been prepared by the Schmidt method.

The cyclic voltammogram of the GC/Nafion/C/MoO_x/Pt electrode in H_2SO_4 showed a redox couple at about 0.45 V vs. RHE, besides the H–adsorption/desorption and PtO formation/reduction usually observed in cyclic voltammograms of Pt in acidic media. The redox peak has been attributed to the MoO_2/MoO_3 couple.

Ioroi et al also estimated the performance of the catalyst toward the oxidation of pure H_2 by employing a membrane electrode assembly (MEA) arrangement. The Pt/Mo/C catalyst prepared under identical experimental conditions gave an efficiency similar to that of Pt/C and PtRu/C.

To investigate the CO tolerance of the three electrocatalysts, oxidation of a CO containing H_2 fuel has been performed. PtRu/C and $Pt/MoO_x/C$ showed comparable efficiencies,[3] which were higher than that reported for Pt/C. The presence of a certain interaction between the Pt sites and the deposited MoO_x has been proposed to explain the reduction of the poisoning effect of CO. The enhancement of the CO_{ads} tolerance that was reported with the $Pt/MoO_x/C$, has been attributed to the activation of the interface between Pt and MoO_x against CO oxidation and modification of the electronic band-structure of Pt.

The improvement reported in the efficiency of the Mo modified Pt electrodes, toward the oxidation of the pure and the CO contaminated H_2, encouraged us to modify a commercial carbon supported Pt catalyst with Mo. In this chapter, the precipitation of MoO_3 onto a 20% Pt commercial catalyst (Etek) was achieved by following the procedure reported by Schrumb and Waterford.[4]

After preparation of ink type electrodes from the Pt/C and the MoO_3 modified Pt/C, the catalytic activity of the electrodes toward the oxidation of methanol and formaldehyde in acidic media was studied by means of cyclic voltammetry. An enhancement of the oxidation current in the presence of MoO_3 was observed for both fuels. It was also found that the oxidation current increases as the amount of the deposited MoO_3 increases to a certain limit, the current then decreases with further elevation in the oxide loading.

5.2 Experimental

5.2.1 Deposition of the MoO_3

The deposition of molybdenum (VI) oxide on a commercial Pt/C catalyst (20% Pt on Vulcan XC-72 carbon, Etek) was performed by the acidification of an ammonium molybdate precursor. In brief, a 200 mL aqueous mixture of ca 0.8 g of ammonium heptamolybdate tetrahydrate (Aldrich) and about 0.2 g of the catalyst was prepared, and brought to boiling with stirring. 100 mL of boiling and concentrated HNO_3 (Fisher Scientific) was then added to the boiling aqueous mixture until a blue precipitate began to appear (MoO_3 is a white substance, it gains its blue color from the co-existence of small amounts of reduced species)[5]. The mixture was then left overnight to cool to room temperature. The product was collected by suction filtration, and then heated in an oven at ca.175 °C for at least 16 hours.

A sample of each dried catalyst was weighed, then it was heated at 550 °C for at least 6 hours to determine its carbon content. The amount of the carbon in the catalyst is the difference between the initial mass and the mass weighed after the combustion at 550 °C. The residue was then heated at 850 °C for 6 other hours to remove the MoO_3. The amount of MoO_3 was estimated as the mass difference between the residue weighed after the first and after the second combustion processes. The Pt content of the catalyst is the difference in mass between the initial weighing and the mass weighed after the second combustion at 850 °C. The gravimetric analysis showed that the method employed

was suitable for the preparation of catalysts with different Pt/MoO_3 ratios. The commercial catalyst was found to contain 18.5% Pt rather than the nominal value of 20%. The accuracy of the gravimetric analysis was confirmed by control experiments using physical mixage of MoO_3 and the commercial catalyst.

5.2.2 Electrode preparation

To prepare inks from the catalysts, the appropriate amount of the catalyst was weighed into a small vial to the desired Platinum loading (60 $\mu g/cm^2$), then 0.45 mL of a 5% by mass Nafion solution in a mixture of lower aliphatic alcohols was added. The suspension was stirred for ca. 2 hours to make homogeneous ink. 1μL of ink was applied to the surface of a previously polished glassy carbon electrode (area = $0.071 cm^2$) and left to dry at room temperature for several hours.

5.3 Results

A Cyclic voltammogram of the MoO_3 modified catalyst is shown in figure 5.1. The H-adsorption/desorption region is fused with a redox wave of significantly higher current density. PtO formation/reduction appears at more positive potentials than these waves.

The MoO_3 modified catalyst was employed for the oxidation of methanol as shown in figure 5.2. A comparison between the voltammetric response of the modified catalyst and that of the original commercial catalyst shows only a slight difference in the onset of the oxidation potential at 0.2 V. In spite of that, the oxidation current generated

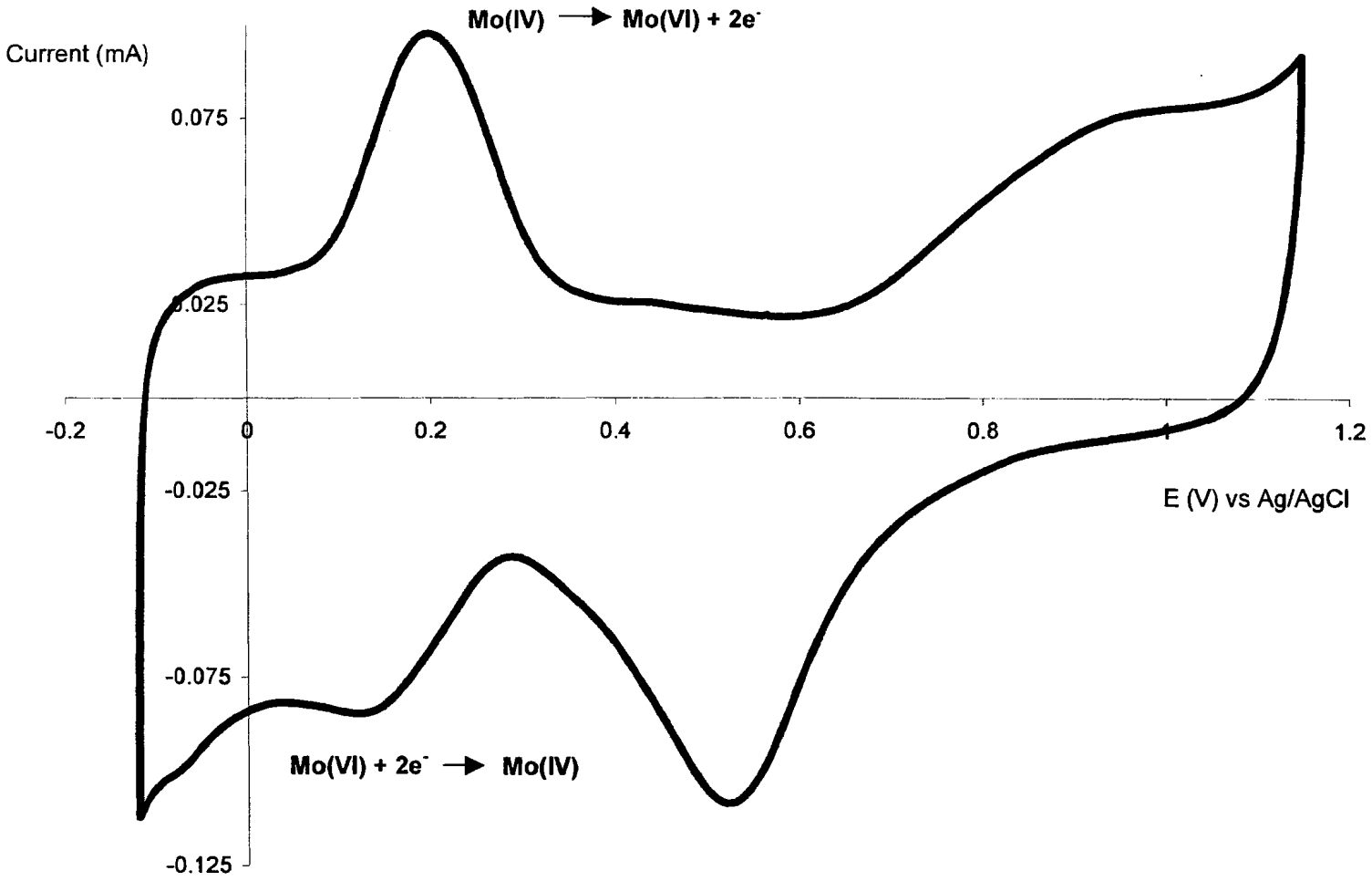

Figure 5.1: Cyclic voltammogram of 13%Pt/31%MoO_3/56%C in 0.5 M H_2SO_4. Scan rate = 20 mVs^{-1}

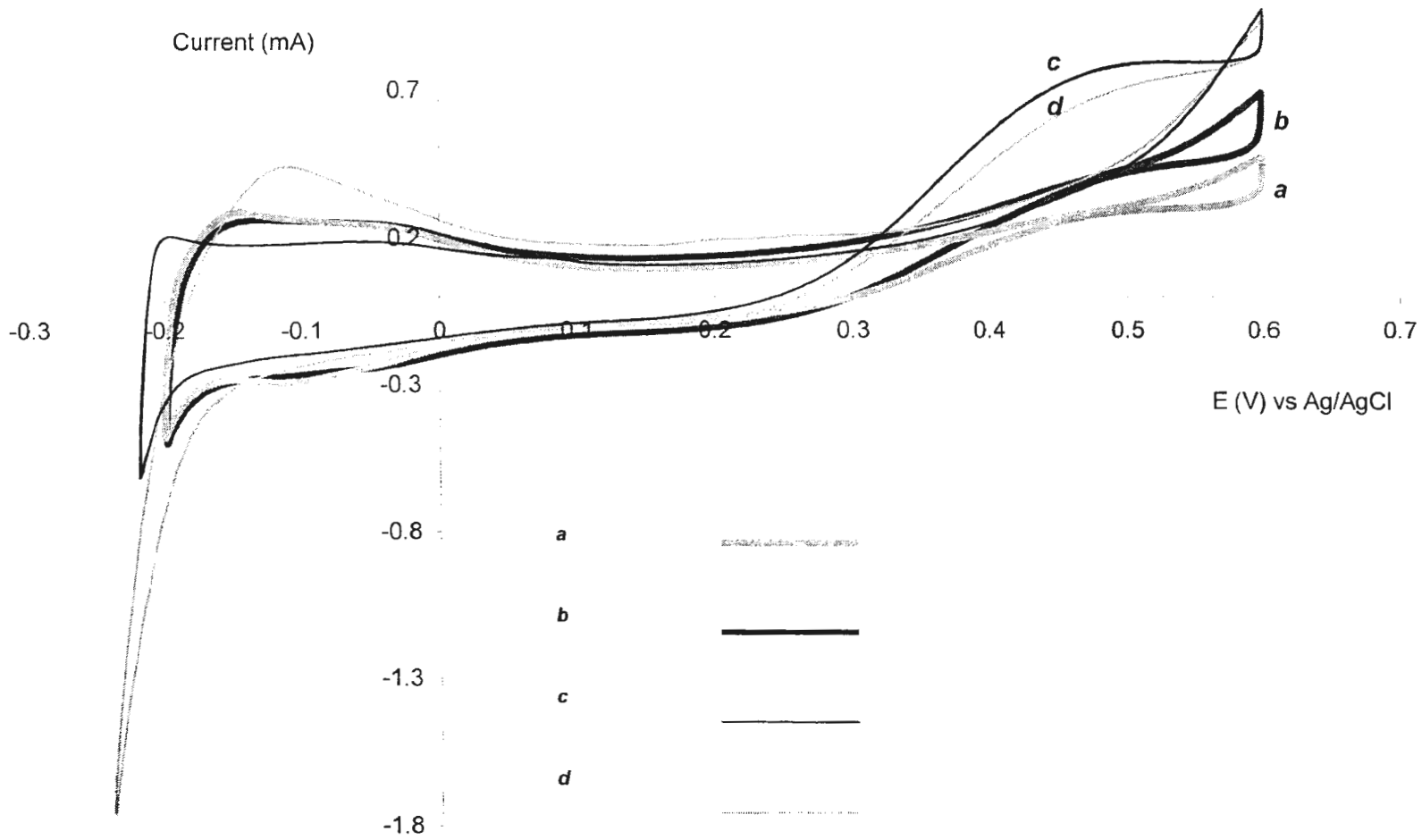

Figure 5.2: Cyclic voltammograms of (a) commercial 20%Pt/80%C (b) 12%Pt/10%MoO_3/78%C (c) 13%Pt/31%MoO_3/56%C (d) 7%Pt/67%MoO_3/26%C in 1M CH_3OH/1M H_2SO_4. Scan rate = 100 mVs^{-1}

at the modified catalyst is higher than that generated on the unmodified catalyst. In addition, it was found that the oxidation current increases with the concentration of MoO_3, to a certain limit. In this work, the maximum efficiency was obtained with 31mass % MoO_3. A comparison between curves c and d in figure 5.2 shows that the current decreases as the MoO_3 loading is increased from 31 to 67 mass %.

Two peaks are observed on extension of the upper limit of the scan from 0.6 to 1.4 V as it is demonstrated in figure 5.3. Peak 1 and Peak 2 occurs during the anodic and the cathodic scans, respectively. To check for any changes in the voltammetric response of the modified catalyst, the upper limit of the scan was returned to 0.6 V. Curves a and b in figure 5.4 represent the cyclic voltammograms that were obtained before and after the extension to 1.4 V, respectively. The two curves are nearly superimposable over the entire scanned potential range.

Figure 5.5 shows cyclic voltammograms of the modified and the commercial catalysts in aqueous $HCHO/H_2SO_4$ solution. About a two-fold enhancement in the oxidation current is observed with the $P/MoO_3/C$ catalyst relative to the Mo free counterpart, especially at potentials more positive than 0.2 V.

A steady state cyclic voltammogram of the modified catalyst in $HCHO/H_2SO_4$ is shown in figure 5.6. Peak 1 and Peak 2 as shown in the figure are observed during the anodic and the cathodic potential scans, respectively. The sharp edge at Peak 2 was reproducible for different electrodes.

Extension of the upper potential scan from 0.6 to 1.4 V limit as shown in figure 5.6 caused a significant deterioration in the efficiency of the MoO_3 modified electrode

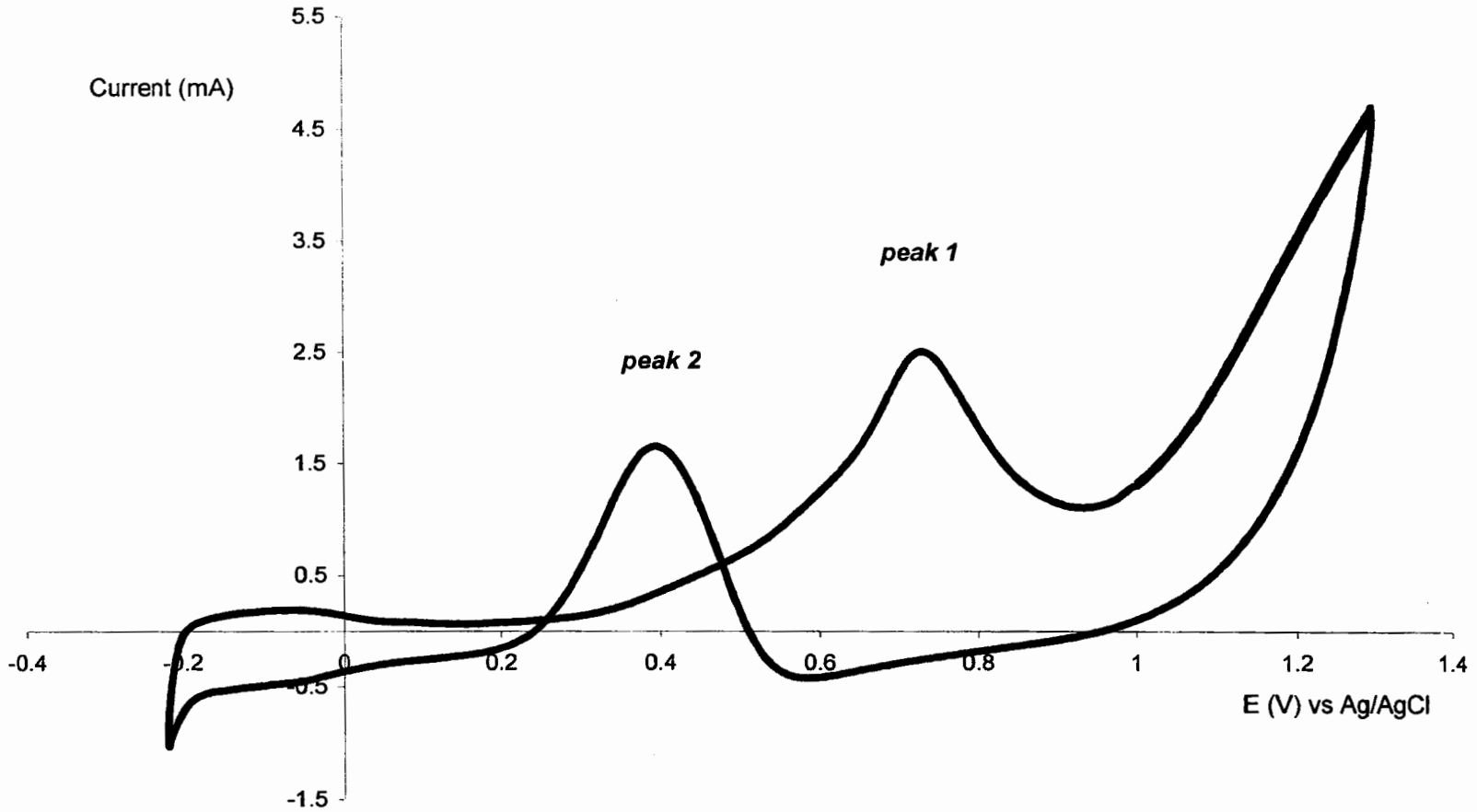

Figure 5.3: Cyclic voltammogram of 13%Pt/31%MoO_3/56% C in 1M CH_3OH/1M H_2SO_4. Scan rate = 100 mVs^{-1}

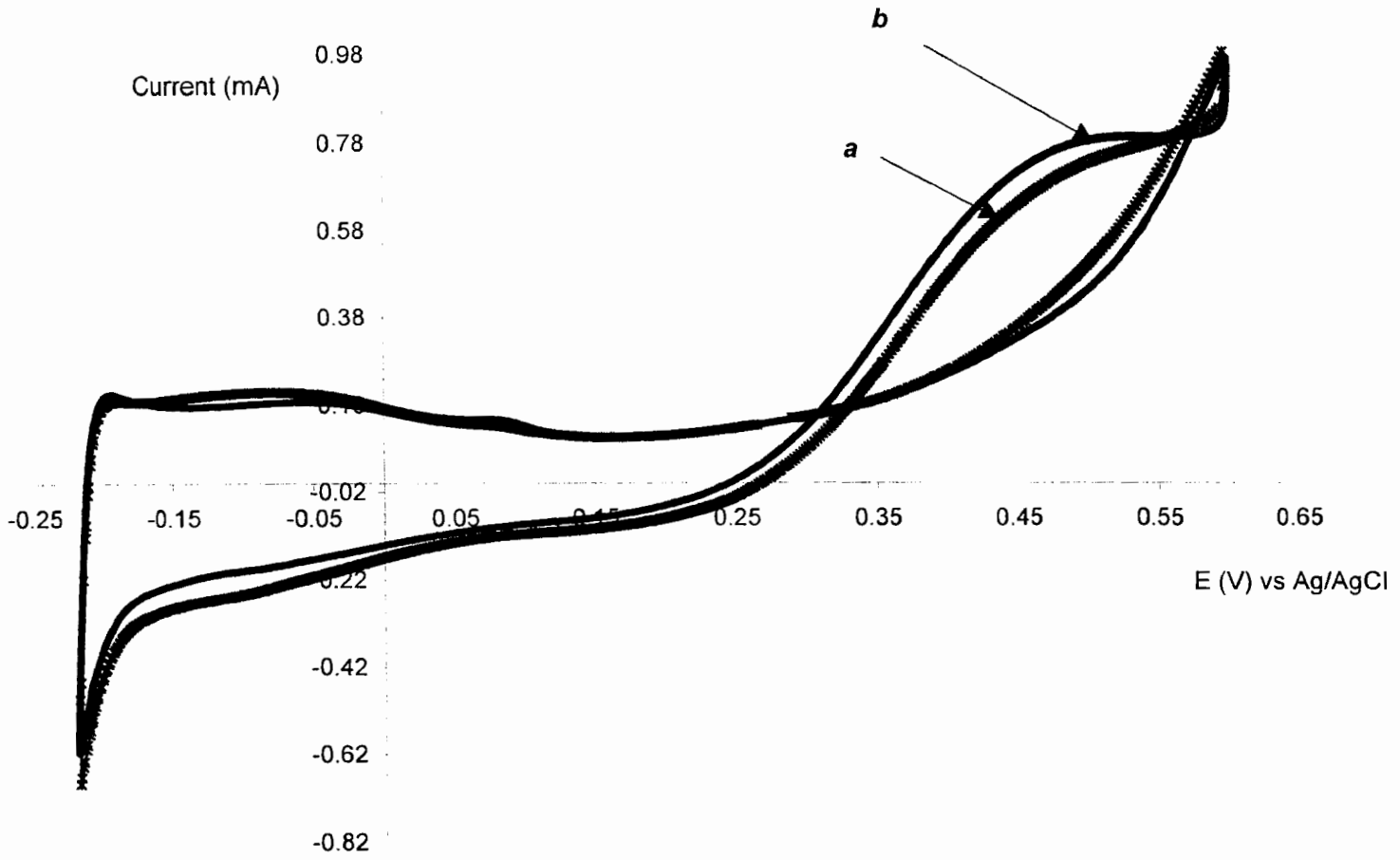

Figure 5.4: Cyclic voltammograms of 13%Pt/31%MoO_3/56%C in 1M CH_3OH/1M H_2SO_4. Scan rate = 100 mVs^{-1}
The scans were taken (a) before and (b) after cycling to an upper limit of 1.4 V

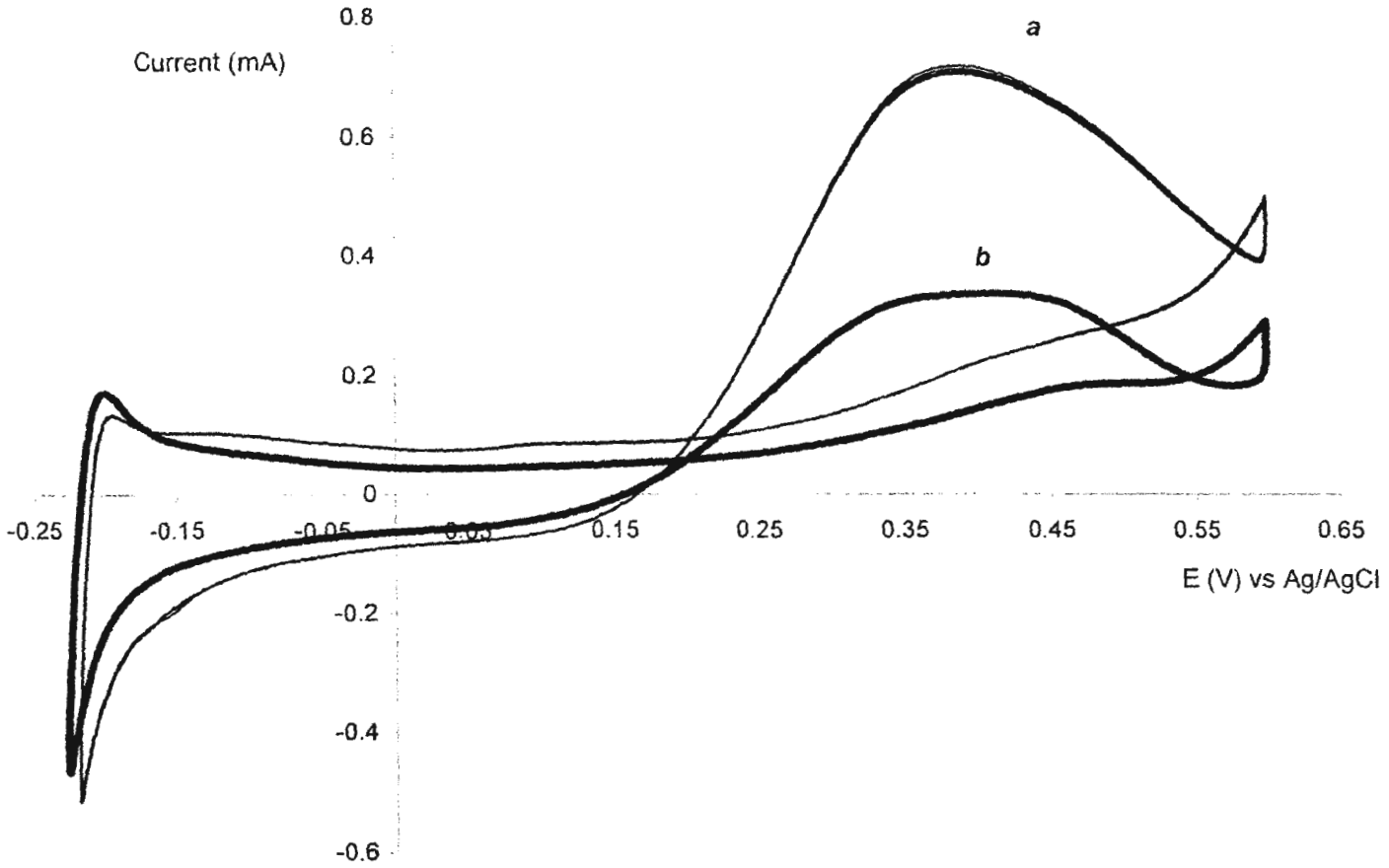

Figure 5.5: Cyclic voltammograms of (a) 13%Pt/31%MoO_3/56%C and (b) commercial 20%Pt/80% C, in 1M HCHO/1M H_2SO_4. Scan rate = 100 mVs^{-1}

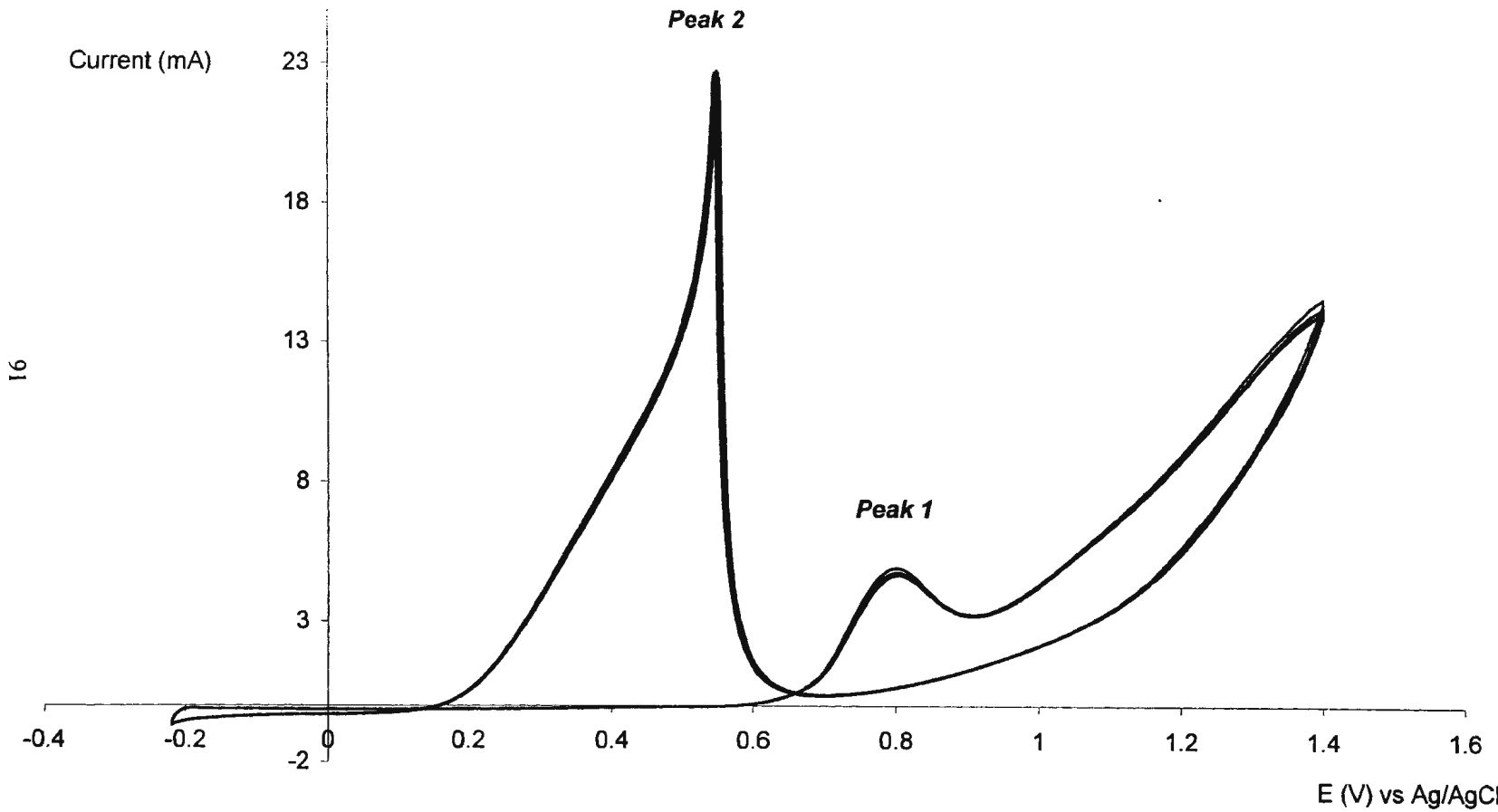

Figure 5.6: Cyclic voltammogram of 13%Pt/31%MoO_3/56%C in 1M HCHO/1M H_2SO_4. Scan rate = 100 mVs^{-1}

toward the oxidation of HCHO. Cyclic voltammograms of the $Pt/MoO_3/C$ electrode from – 0.2 V to 0.6 V, before and after the extension of the upper potential scan limit to 1.4 V are represented by curves a and b in figure 5.7, respectively. The oxidation peak in curve b, at about 0.4 V, is approximately ½ of that observed in curve a.

5.4Discussion

5.4.1 The electrochemical behavior of $Pt/MoO_3/C$ in H_2SO_4 aqueous solution.

The redox couple shown in figure 5.1 at ca. 0.2 V can be attributed to the MoO_2/MoO_3 pair. The same electrochemical feature has been observed in cyclic voltammograms of the $Pt/MoO_x/C$ catalysts prepared by electrochemical deposition or chemical reduction methods.[3,6] The electrochemical reaction of the Mo(VI)/Mo(IV) redox couple can be written as:

$$Mo(VI) + 2e^- \rightleftharpoons Mo(IV) \qquad (5.1)$$

The relatively high currents that accompany this electrochemical reaction in figure 5.1 can be attributed to the high loading of the precipitated MoO_3. With the $Pt/MoO_x/C$ catalyst prepared by Ioroi et al,[3] the nominal Mo content was about 9% by mass. In that work, the currents that have been attributed to the electrochemical reaction represented by equation 5.1 were approximately ½ of the currents observed in the H-adsorption/ desorption region.

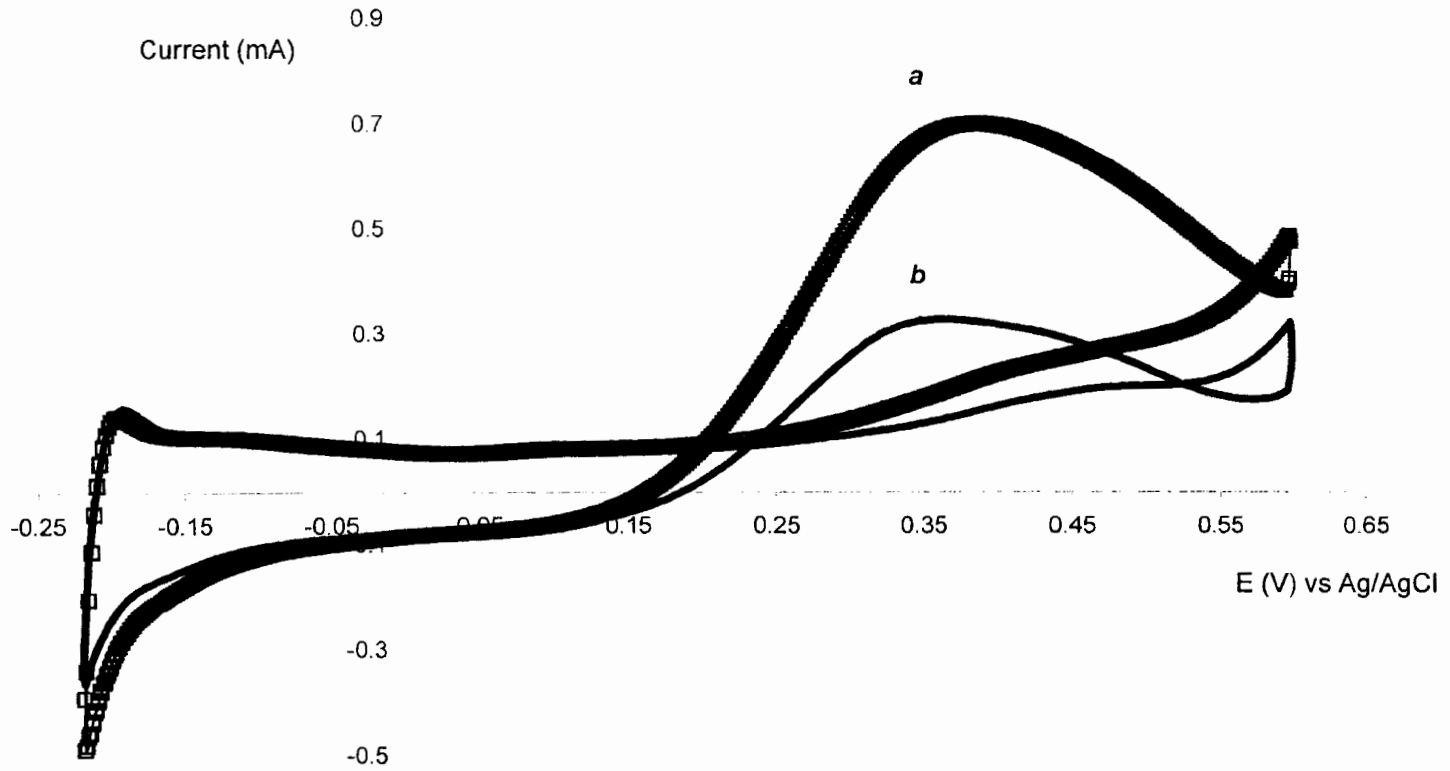

Figure 5.7: Cyclic voltammograms of 13%Pt/31%MoO_3/56%C in 1M HCHO/1M H_2SO_4. Scan rate = 100 mVs^{-1}.The scans were taken (a) before and (b) after cycling to an upper limit of 1.4 V

The $Pt/MoO_3/C$ modified electrodes prepared in this work showed stability toward potential cycling in aqueous H_2SO_4. The cyclic voltammogram shown in figure 5.1 was recorded after at least 50 cycles in the acidic medium.

5.4.2 The oxidation of methanol

The catalytic promotion that was reported after modification of the commercial Pt/C catalyst with MoO_3 can be explained by the bi-functional mechanism proposed by Watanabe and Motoo.[7] The dispersed MoO_3 has the ability to split water molecules at potentials lower than that reported for Pt. Adsorbed hydroxyl groups are generated from the dissociation reaction, as shown in equation 5.2:

$$Pt + MoO_3 + H_2O \rightleftharpoons MoO_3\text{–}OH_{ads} + Pt\text{–}H_{ads} \qquad (5.2)$$

The hydroxyl groups activate the oxidative conversion of CO_{ads} to CO_2 as:

$$Pt\text{–}CO_{ads} + MoO_3\text{–}OH_{ads} \rightleftharpoons CO_2 + H^+ + Pt + MoO_3 + e^- \qquad (5.3)$$

It was found that the oxidation current decreases by increasing the MoO_3 concentration from 31 to 67 mass %. At higher MoO_3 concentrations, the dispersed metal oxide may block the active Pt sites where the dissociation and oxidation of methanol takes place. The high MoO_3 content may also reduce the electronic conductivity of the catalyst that is mainly due to the carbon support. The carbon content of the 67 mass % MoO_3 catalyst is the lowest among all the catalysts that were studied in this work.

Peak 1 shown in figure 5.3 was attributed to a combination of different oxidation processes; mainly the oxidation of methanol, as well as the oxidation of adsorbed intermediates produced from its dissociation on the Pt sites. Contributions from PtO

formation and to some extent the direct oxidation of methanol to CO_2 were also considered. Similar results were obtained by Li et al,[8] who attributed the oxidation peak reported during the backward scan, Peak 2, to the oxidation of methanol on a clean Pt sites after the reduction of the PtO from the electrode's surface.

Shropshire[9] reported that a molybdate thin film adsorbed on the surface of Pt black was lost at high positive potentials, and replaced with a layer of adsorbed methanol molecules. The stability of the modified catalyst prepared in this work toward scanning the potential to an upper potential scan limit of 1.4 V was therefore investigated.

Figure 5.4 shows that the dispersed MoO_3 has not been removed from the electrode's surface at higher positive potentials. The voltammetric response from the $Pt/MoO_3/C$ before and after the scanning to the mentioned upper scan limit are almost the same, indicating the preparation of a catalyst of significant structure stability, at least for the purposes of methanol oxidation. Further experimental investigation is required to reveal the nature of the unexpected retention in activity.

5.4.3 The oxidation of formaldehyde

It was found that the catalytic activity of the $Pt/MoO_3/C$ catalyst relative to its Pt/C counterpart, toward the oxidation of formaldehyde is similar to that observed for the oxidation of methanol. The two-fold enhancement, toward the oxidation of HCHO, shown in figure 5.5 at potentials more positive than 0.2 V can be explained in terms of the bi-functional mechanism.

The oxidation of formaldehyde on a polycrystalline Pt electrode has been reported by Olivi et al.[10] Two oxidation peaks have been reported in the cyclic voltammogram of the Pt electrode in aqueous $HCHO/HClO_4$. The first peak has been reported during the forward scan at a potential of ca. 0.77 V. This peak has been attributed to the dissociation of formaldehyde into several forms of CO_{ads}. The formation of linearly-bonded, bridged-bonded, and multibonded CO_{ads} species has been monitored by electromodulated infrared reflectance spectroscopy (EMIRS). The second oxidation peak appeared during the cathodic scan after the reduction of Pt oxide and has been attributed to the oxidation of formaldehyde on a CO_{ads} free Pt surface.

The two peaks reported by Oliviri and co-workers were also observed in this work. Peak 1 at ca. 0.8 V can be attributed to the adsorptive dissociation of formaldehyde on the Pt sites of the prepared $Pt/MoO_3/C$. Investigation of the nature of the species produced from the dissociation process is beyond the scope of our work.

Peak 2 shown in figure 5.6 was attributed to the direct oxidation of formaldehyde on clean Pt sites after the removal of the PtO layer. Further experimental investigation is required to discover the origin of the edge observed at top of peak 2 in figure 5.6.

The loss of the catalytic activity toward formaldehyde oxidation with extension of the upper limit may be due to replacement of adsorbed MoO_3 by formaldehyde, as proposed for methanol by Shropshire.[9] Curve b in figure 5.7 is the voltammogram of the MoO_3 modified electrode that was taken after the reduction of the upper limit of the scan from 1.4 to 0.6 V. The electrochemical features shown in Curve b, figure 5.7, are similar to those of the unmodified Pt/C catalyst prepared in this work.

5.5 Conclusion

A commercial carbon supported catalyst was modified with MoO_3. Ink type electrodes prepared from the commercial and modified catalysts were examined for the oxidation of methanol and formaldehyde. With both fuels, the modified catalyst showed a higher catalytic performance than the original commercial catalyst. The catalytic activity was explained in terms of the bi-functional mechanism.

The modified catalyst showed a reproducible voltammetric response when it was tested for methanol oxidation. With formaldehyde, scanning the potential of the electrode to higher positive potentials was accompanied with the removal of the deposited MoO_3.

List of references

[1] Shukla, A. K.; Ravikumar, M. K.; Arico, A. S.; Candiano, G.; Antonucci, V.; Giordano, N.; Hamnett, A. *J. Appl. Electrochem.* ***1995***, 25, 528-532.

[2] Mukerjee, S.; Lee, S. J.; Ticianelli, E. A.; McBreen, J.; Grgur, B. N.; Marcovic, N. M.; Ross, P. N.; Giallombardo, J. R.; De Castro, E. S. *Electrochem. Solid-State Lett.* ***1999***, *2*, 12-15.

[3] Ioroi, T.; Fujiwara N.; Siroma, Z.; Yasuda, K.; Miyazaki, Y. *Electrochem. Commun.* ***2002***, *4*, 442-446.

[4] Schumb, W.; Hartford, W. H. *J. Am. Chem. Soc.* ***1934***, *56*, 2613-2615.

[5] Busev, A.I., In *Analytical Chemistry of Molybdenum;* Ann Arbour-Humphrey Science Publishers; Ann Arbor, ***1969***, p 137.

[6] Wang, Y.; Fachini, E. R.; Cruz, G.; Zhu, Y.; Ishikawa, Y.; Colucci, J. A.; Cabrera, C. R. *J. Electrochem. Soc.* ***2001***, *148*, C222-C226.

[7] Watanabe, M.; Motoo, S. *Electroanal. Chem.* ***1975***, *60*, 267-273.

[8] Li, W. S.; Tian, L. P.; Li, H. H.; Chen, H. Y.; Lian, X. P. *J. Power Sources* ***2002***, *104*, 281-288.

[9] Shropshire, J. A. *J. Electrochem. Soc.* ***1965***, *112*, 465-469.

[10] Olivi, P.; Bulhöes, L. O. S.; Léger, J.-M.; Hahn, F.; Baden, B.; Lamy, C. *J. Electroanal. Chem.* ***1994***, *370*, 241-249.

Chapter 6

Summary

Enhancement of the catalytic activity of a polycrystalline Pt electrode toward the oxidation of methanol and formaldehyde, upon modification with Mo oxides showed that both of the hydrogen molybdenum bronzes, H_xMoO_3, and the molybdenum oxides, MoO_x, catalyze the oxidation reaction at the Pt surface.

The main difference between the two Mo compounds is the manner of preparation. The preparation of the bronzes was conducted in an *in situ* fashion, by the application of potentials more negative than 0 vs. Ag/AgCl to a polycrystalline Pt electrode in $MoO_4^{2-}/CH_3OH/H_2SO_4$ aqueous solution. The formation of a green layer has been witnessed visually and has been attributed to the $(H_2MoO_3)_{ads}$ bronze. The generated bronze undergoes at least two oxidation processes at higher positive potentials.

The first oxidized intermediate generated at 0.3 V enhances the dissociation of methanol at a potential which is more negative by 0.2 V than that observed with the unmodified Pt electrode. The second intermediate is produced at ca. 1.1 V. It catalyzes the direct oxidation of methanol to CO_2 with the generation of higher anodic currents.

The nature of the interaction between the adsorbed intermediates and methanol needs further experimental work. Future work may include hydrodynamic voltammetric experiments needed to investigate the kinetics of the oxidation process at the Mo modified electrode.

The ink methodology has been found to be fruitful in the preparation of mechanically stable electrodes. The preparation of carbon supported ink type electrodes is reported in this thesis. Two kinds of supported catalysts were examined for the oxidation of methanol and formaldehyde. The catalytic activity of a MoO_3 modified catalyst relative to its Mo free counterpart is reported. The modified catalyst provides a two fold increase in the oxidation current, especially in the potential range from 0.2 to 0.6 V.

To account for the catalytic improvement that was obtained, the bi-functional mechanism model was employed. The formation of oxygen containing species bonded to the surface MoO_3 was proposed. The oxygenated particles activate the oxidative removal of CO_{ads} from the neighboring Pt sites.

The oxidation of methanol at the modified catalyst was found dependent on the loading of the deposited MoO_3. The oxidation current increases with the elevation of the oxide concentration to 31mass %. Then it decreases with further addition of the oxide. To explain this behavior, it was proposed that at higher Mo loading, the oxide blocks the Pt sites from the methanol. As a consequence, the oxidation rate decreases as it was found in going from 31 to 67 mass % MoO_3.

As the content of the deposited Mo oxide content increases, the concentration of the corresponding carbon support decreases. The role of the carbon support in electron conductivity was discussed within the context of this thesis, especially in Chapter 3. Reduction of the carbon content in the $Pt/MoO_3/C$ may decrease its conductivity, and this should be investigated.

The work reported in this thesis provides a preliminary comparison between the molybdenum- modified electrodes and their unmodified counterparts. Estimation of the commercial value of the modified catalysts, for fuel cells purposes, needs further electrochemical examination. Chronoamperometric analysis and fuel cells test would reveal the longer term activity of the modified catalysts. In addition, coupling of electrochemical techniques with optical methods would be helpful in providing real time monitoring of the species that are produced during the electrochemical reaction under investigation.